breath-hold. The volume data set was acquired in helical mode (64 × 0.625 mm collimation; CT pitch factor, 0.18 to 0.24:1; tube current, 600 to 750 mA with ECG-correlated tube current modulation; tube voltage, 120 kV). The effective radiation dose was estimated on the basis of the dose-length product and ranged from 15 to 18 mSv (5). Image reconstruction was performed with image-analysis software (CardIQ, GE Healthcare) on a dedicated computer workstation (Advantage Workstation Ver.4.2, GE Healthcare). A "standard" kernel was used as the reconstruction filter. Depending on heart rate, either a half-scan (temporal window = 175 ms) or multi-segment (temporal window <175 ms) reconstruction algorithm was selected, and the optimal cardiac phase with the least motion artifacts was chosen individually.

Evaluation of NCP characteristics. All coronary segments >2 mm in diameter were evaluated by 2 blinded and independent observers with curved multiplanar reconstructions and cross-sectional images rendered perpendicular to the vessel center line. The definitions of NCPs and coronary calcium were as follows (5): NCP: a low-density mass >1 mm^2 in size, located within the vessel wall and clearly distinguishable from the contrast-enhanced coronary lumen and the surrounding pericardial tissue; coronary calcium: a structure on the vessel wall with a CT density above that of the contrast-enhanced coronary lumen or with a CT density of >120 Hounsfield units (HU) assigned to the coronary artery wall in a plain image. For NCPs and calcium analyses, the optimal image display setting was chosen on an individual basis; in general, the window was between 700 and 1,000 HU, and the level between 100 and 200 HU.

As previously described ( ), we determined the minimum CT density in each NCP by placing at least 5 regions of interest (area = 1 mm^2) in each lesion and documenting the lowest average value of all regions of interest, and on the basis of our previous results ( ), low-density NCPs were defined as lesions with a minimum CT density of <40 HU. We also determined the extent of luminal enhancement of each coronary lesion by placing a region of interest (area = 1 mm^2) in the center of the coronary artery lumen at the respective reference segment. On the basis of measurements of the cross-sectional vessel areas (mm^2) at each NCP site of maximum vessel area and each proximal reference site of the same coronary artery, we calculated the "Remodeling Index" (RI). Positive remodeling was defined as RI >1.05 ( ). Finally, we assessed calcium deposits in or adjacent to each NCP by determining their presence or absence and their morphology. Spotty calcium was defined as follows: length of calcium burden <3/2 of vessel diameter and width <2/3 of vessel diameter (8). If the initial classification of NCP and adjacent calcium differed among the 2 independent observers, final classification was achieved by consensus.

Statistical analysis. Coronary calcium score is expressed as median value and range, and other measurements are expressed as mean ± SD. Continuous and categorical variables were compared with the Mann-Whitney test and chi-square test, respectively. Interobserver variability of measured CT densities and cross-sectional vessel areas was determined by calculating Pearson's correlation coefficient. In comparisons between ACS and non-ACS lesions and culprit and nonculprit lesions, we used only lesion specific factors, not including patient characteristics because lesions clustered in a single patient. Parameters of NCPs were tested with a receiver-operator characteristic curve to assess their reliability as prognostic variables for predicting ACS culprit lesions. Logistic regression was used to examine the associations between NCP characteristics (RI, presence of adjacent spotty calcium, NCP CT density, and reference site CT density) and ACS culprit lesions for multivariate analysis adjusted for the location of NCPs. All analyses were done with JMP 5.0.1 statistical software (SAS Institute Inc., Cary, North Carolina). A p value of <0.05 was considered statistically significant.

RESULTS

Baseline characteristics. The mean heart rate during scanning was 61 ± 10 beats/min; mean scan time for coronary CT angiography was 6.3 ± 2.1 s. No patient experienced any complication due to MDCT, and no patient was excluded from analysis due to poor image quality of the 64-slice CT.

Of the 147 patients, 46 (31%) had no NCPs as detected by 64-slice CT angiography (31 patients had no coronary atherosclerotic lesions, and 15 patients had only calcified coronary lesions), and all 46 had presented with stable symptoms. In the remaining 101 patients (69%) (21 patients with ACS [8 NSTEMI and 13 unstable anginas] and 80 of 126 patients with stable clinical presentation [non-ACS: no symptom, atypical chest pain, or stable exertional chest pain]), CT angiography allowed detection of at least 1 coronary lesion that contained noncalcified components. A total of 228 NCPs were visualized (on average, 2.2 ± 1.2/patient; range, 1 to 5 lesions/patient). Clinical

JACC: CARDIOVASCULAR IMAGING, VOL. 2, NO. 2, 2009
FEBRUARY 2009:153–60

Table 1. Patients' Characteristics

	ACS Group (n = 21)	Non-ACS Group (n = 80)	p Value
Age (yrs)	66 ± 11	69 ± 9	NS
Male/female	17/4	61/19	NS
Hypertension	13 (62)	53 (66)	NS
Hyperlipidemia	12 (57)	37 (46)	NS
Diabetes mellitus	8 (38)	39 (49)	NS
Previous or current smoker	12 (57)	45 (56)	NS
Statin use	8 (38)	23 (29)	NS
Heart rate (beats/min)	59 ± 7	59 ± 9	NS
Body mass index (kg/m^2)	25 ± 3	24 ± 4	NS
Coronary calcium score	184 (0–1,550)	107 (0–4,656)	NS

N = 101. Coronary calcium score is expressed as median value (range). Other data are the mean value ± SD or n (%) of patients.
ACS = acute coronary syndrome.

characteristics of the 101 patients with NCPs are shown in Table 1. There were no statistically significant differences between ACS and non-ACS groups. Figure 1 shows MDCT and invasive angiographic findings in a case with ACS.

Comparisons of NCP findings between ACS and non-ACS patients. Sixty-five and 163 NCPs were detected in the ACS (n = 21) and non-ACS (n = 80) group, respectively. The location of NCPs in the ACS and non-ACS groups was similar (6% and 10% in the left main coronary artery, 37% and 39% in the left anterior descending artery, 20% and 15% in the left circumflex artery, 37% and 36% in the right coronary artery, respectively). The mean number of NCPs/patient was significantly higher in the ACS group (3.1 ± 1.2) than in the non-ACS group (2.0 ± 1.1, $p < 0.01$). Comparisons of NCP characteristics between the 2 groups are shown in Table 2. Excellent inter-observer agreement was found for minimum CT densities of NCPs ($r = 0.91$), for luminal densities at the reference site lumens ($r = 0.94$), and for all cross-sectional vessel areas ($r = 0.88$). The minimum CT density of NCPs was significantly lower in the ACS group (24 ± 22 HU) than in the non-ACS group (42 ± 29 HU, $p < 0.01$). There was no difference in mean CT densities of reference site lumens between the ACS and non-ACS groups. The mean RI of NCPs was significantly higher in the ACS group than in the non-ACS group (1.14 ± 0.18 vs. 1.08 ± 0.19, $p = 0.02$). Noncalcified coronary atherosclerotic plaques were more frequently associated with spotty calcification in the ACS group (60%) as compared with the non-ACS group (38%, $p < 0.01$). Furthermore, the frequency of low-density NCPs with PR and spotty calcium was substantially higher in the ACS group (43%) than in the non-ACS group (22%, $p < 0.01$).

CT characteristics of culprit versus nonculprit lesions in ACS patients. In the 21 ACS patients, 21 culprit and 44 nonculprit NCPs were detected. Of these lesions, 32 (21 culprit and 11 nonculprit) were assessed as obstructive (>50% stenosis) by invasive angiography. Comparisons of NCP characteristics between culprit and nonculprit lesions in the ACS group are shown in Table 3. The frequency of adjacent spotty calcium was similar in both types of plaques (57% vs. 61%). The minimum CT density of the culprit lesions tended to be lower than that of the nonculprit lesions (15 ± 13 HU vs. 28 ± 24 HU), but this difference did not reach statistical significance. The mean RI of the culprit lesions (1.26 ± 0.16) was significantly higher than that of the nonculprit lesions (1.09 ± 0.17, $p < 0.01$), but there was a substantial overlap of the distribution of RI values in these 2 groups of lesions (Fig. 2). The optimal cutoff for RI by CT angiography to predict culprit lesions was 1.23 and had a sensitivity of 71% and specificity of 82% (area under the curve 0.77). The frequency of plaques that displayed all 3 parameters of "vulnerability" (low CT density, positive remodeling, and spotty calcium) tended to be higher for culprit lesions (57%) compared with nonculprit lesions (36%). However, the difference was not significant. Multivariate analysis, which included larger RI (≥1.23), the presence of adjacent spotty calcium, the minimum NCP CT density, and the reference site CT density, revealed that a larger RI was the only significant predictor of ACS culprit lesions (odds ratio: 12.3; 95% confidence interval: 2.9 to 68.7, $p < 0.01$). Furthermore, the mean RI of the 21 culprit lesions was significantly higher than that of the 11 obstructive nonculprit lesions (1.26 ± 0.16 vs. 1.08 ± 0.16, $p < 0.01$), whereas the minimum CT densities (15 ± 13 HU vs. 15 ± 18 HU), frequencies of adjacent spotty calcium (57% vs. 64%), and frequencies of low-density NCPs with PR and spotty calcium (57% vs. 45%) were similar.

DISCUSSION

In this study, we demonstrated that 64-slice CT coronary angiography allows visualization of more noncalcified coronary atherosclerotic lesions with characteristics assumed to be associated with plaque "vulnerability" in patients with ACS as compared with patients with stable clinical presentation. Thus, 64-slice CT might contribute toward the differentiation of "vulnerable patients." Furthermore, we observed that a high degree of positive remodeling is the most

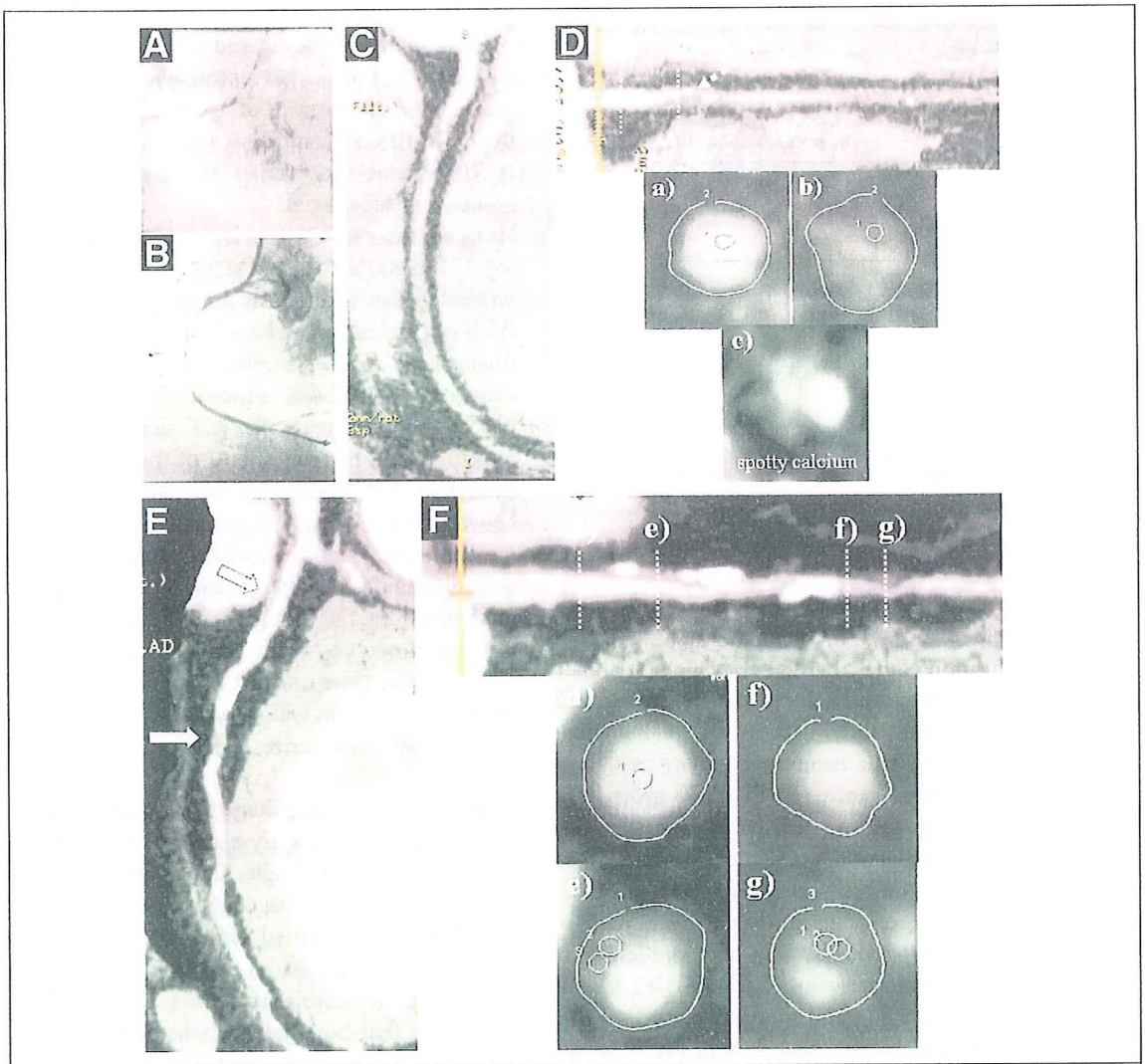

Invasive Angiography and Coronary CT Angiography in a 58-Year-Old Man With NSTEMI

(A and B) Invasive coronary angiographic images show an initial occlusion of the proximal portion of the right coronary artery (RCA) (arrowhead) and a recanalization of the lesion. (C and D) Curved multiplanar reconstruction (MPR) images show the subtotal occlusion and noncalcified coronary atherosclerotic plaque (NCP) with spotty calcium in the proximal portion of the RCA (arrowhead). The cross-sectional vessel areas of the reference site (a) and NCP (b) are 23 and 29 mm^2, respectively. Therefore, the remodeling index (RI) is 1.26. The minimum computed tomography (CT) density of the NCP is 16 Hounsfield units (HU) (b). Spotty calcium with the NCP is observed in the cross-sectional image (c). (E and F) Curved MPR images show multiple nonculprit NCP in left anterior descending coronary artery (LAD) (arrows). The cross-sectional vessel areas of the reference site (d) and nonobstructive NCP (e) in the proximal portion are 28 and 28 mm^2, respectively. Therefore, the RI is 1.0. The minimum CT density of the NCP is 44 HU (e). The cross-sectional vessel areas of the reference site (f) and obstructive NCP (g) in the middle portion are 18 and 18 mm^2, respectively. Therefore, the RI is 1.0. The minimum CT density of the NCP is −7 HU (g). NSTEMI = non–ST-segment elevation myocardial infarction.

accurate discriminator of culprit and nonculprit lesions in ACS patients. Thus, our results provide further evidence for the potential of MDCT angiography to noninvasively identify vulnerable lesions and vulnerable patients.

General findings of NCPs in ACS. In a report using 16-slice CT angiography, the prevalence of noncalcified plaque was 100% in ACS culprit lesions (3). The present study on 64-slice CT also confirms the presence of NCPs in all ACS patients and in all ACS culprit lesions, whereas no patient without any NCP had an ACS. Although the number of ACS patients was small (n = 21), this indicates a high sensitivity of NCP as detected by CT to identify patients with ACS.

Furthermore, our findings are in accordance with previous evidence that the disease process in ACS patients is not focal but more widespread throughout

JACC: CARDIOVASCULAR IMAGING, VOL. 2, NO. 2, 2009
FEBRUARY 2009:153–60

Table 2. Comparison of NCP Characteristics Between ACS and Non-ACS Groups

	ACS Group (n = 65)	Non-ACS Group (n = 163)	p Value
CT density (HU)			
NCPs (minimum density)	24 ± 22	42 ± 29	< 0.01
Reference site	351 ± 44	357 ± 62	0.46
Remodeling index	1.14 ± 0.18	1.08 ± 0.19	0.02
Adjacent spotty calcium, (n [%])	39 (60)	62 (38)	< 0.01
Low-density NCPs (<40 HU) with PR and spotty calcium, (n [%])	28 (43)	36 (22)	< 0.01

Data are the mean value ± SD or n (%) of non-calcified coronary atherosclerotic plaque (NCPs).
ACS = acute coronary syndrome; CT = computed tomography; HU = Hounsfield units; PR = positive remodeling.

the coronary circulation and might lead to instability of multiple plaques (9). In fact, multiple plaque ruptures in locations other than on the culprit lesion have been detected by IVUS in patients with ACS (10). In the present study, with 64-slice CT angiography that can evaluate the entire coronary tree, more NCPs/patient were detected in the ACS group than the non-ACS group, and those that were detected more frequently displayed "vulnerable" characteristics, such as lower CT density, extent of arterial remodeling, and presence of adjacent spotty calcium. Motoyama et al. (1) reported that 47% of culprit lesions in ACS had all 3 characteristics of PR (RI >1.1), low CT density (<30 HU), and spotty calcium (<3 mm in size). We also observed that 43% of NCPs in the ACS group had all 3 vulnerable characteristics, although the criteria we used varied slightly. This indicates that multiple vulnerable plaques with characteristics similar to the culprit lesion are often present in the entire coronary tree of ACS patients.

Predictors of ACS culprit lesions in MDCT. A previous study with CT angiography (4) revealed that, among the 3 vulnerable characteristics, positive remodeling was the strongest discriminator between culprit and nonculprit lesions in patients with ACS (PR: 87%; low CT density: 79%; spotty calcium: 63%), similar to our results. Whereas this could be explained by previous data, such as a histopathological study using postmortem hearts that revealed that coronary plaques with PR had a higher lipid content and a higher macrophage count (11), or the fact that excessive expansive remodeling promotes continued local lipid accumulation, inflammation, oxidative stress, matrix breakdown, and eventually further plaque progression (12), this observation has to be interpreted with caution. In a retrospective analysis such as ours, the correlation of remodeling and culprit lesions might be a consequence of plaque rupture and not necessarily a predictor. Also, in spite of a significant difference of the mean RI between culprit and nonculprit lesions of ACS patients, the overlap of RI values in these 2 groups was substantial.

Study limitations. Caution is required when interpreting CT densities of NCPs. We cannot exclude the possibility that thrombosis might be present in some ACS culprit lesions, and low-density NCPs are indistinguishable from thromboses due to their similar densities. Thrombosis adjacent to very-low-density NCPs might increase the CT densities that were measured, and this might be 1 of the reasons that the minimum CT density is not statistically different between the culprit and nonculprit lesions in the present study. We believe that selecting the minimum density value as the NCP density is an appropriate method for limiting partial volume and beam hardening effects resulting from neighboring structures, especially hyperdense calcium. However, improvements of spatial resolution will be necessary to more reliably identify and characterize NCPs on the basis of CT densities.

Second, at present, there is no gold standard for determination of coronary plaque vulnerability in CT angiography. For example, in the previous MDCT study, spotty calcium was defined as <3 mm in size (4). However, the visual estimation of high-density structures, such as calcium deposits, varies depending on the window setting in the CT image. Therefore, we believe that our method, which is based on the comparison of calcium dimensions with vessel diameters, is more appropriate for classification of calcium deposits.

Comparison of NCP Characteristics Between Culprit and Non-Culprit Lesions in ACS Group

	Culprit Lesions (n = 21)	Non-Culprit Lesions (n = 44)	p Value
CT density (HU)			
NCPs (minimum density)	15 ± 13	28 ± 24	0.07
Reference site	353 ± 46	350 ± 43	0.95
Remodeling index	1.26 ± 0.16	1.09 ± 0.17	< 0.01
Adjacent spotty calcium, (n [%])	12 (57)	27 (61)	0.75
Low-density NCPs (<40 HU) with PR and spotty calcium, (n [%])	12 (57)	16 (36)	0.11

Data are the mean value ± SD or n (%) of NCPs.
Abbreviations as Table 2.

Third, the present study is retrospectively designed, and we assume that vulnerable NCPs have morphological characteristics similar to those of already-disrupted NCPs—a limitation shared with previous studies in this field. A long-term, large prospective trial would be necessary to determine whether CT stratification of NCPs indeed has prognostic value for predicting future cardiac events. Future approaches might, in fact, extend beyond CT analysis of plaque morphology, such as demonstrated by a recent report that described the use of a dedicated contrast agent to visualize macrophage infiltration in atherosclerotic plaques (15).

Finally, our data acquisition protocol led to a relatively high radiation dose for coronary CT angiography. Recently, a prospectively ECG-triggered algorithm has been developed that allows imaging with substantially reduced dose (14). Further studies will be required to validate the accuracy for identification and characterization of NCPs with newer low-dose algorithms.

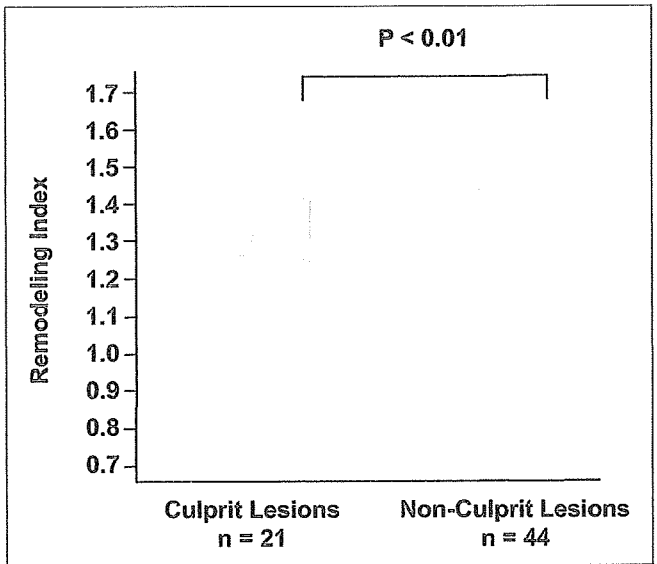

Figure 2. Comparison of RI Between ACS Culprit and Nonculprit Lesions

The mean RI of the culprit lesions is significantly higher than that of the non-culprit lesions (1.26 ± 0.16 vs. 1.09 ± 0.17, $p < 0.01$), but there is a substantial overlap of the distribution of RI values in these 2 groups of lesions. ACS = acute coronary syndrome; RI = remodeling index.

CONCLUSIONS

We were able to demonstrate that 64-slice coronary CT angiography detects a higher number of atherosclerotic lesions with noncalcified components in patients with ACS as compared with patients with stable symptoms. Identifying the actual culprit lesion in ACS patients is more difficult: among the characteristics that are assumed to be associated with plaque "vulnerability" in CT, a large degree of positive remodeling was the only independent predictor of culprit lesions in ACS patients, but a large variability was observed concerning the extent of positive remodeling in culprit and nonculprit lesions. Rather than identifying a single lesion responsible for a future coronary event, the ability to investigate plaque characteristics throughout the entire coronary system in a noninvasive fashion might be an important property of coronary CT angiography regarding its potential application in the context of identifying "vulnerable patients" at risk for ACS.

Acknowledgments

The authors are grateful to Nobuhiko Hirai, MD, and Masao Kiguchi, RT, for their technical assistance. The authors also thank Dr. Shozo Miki for his critical reading of the manuscript.

Reprint requests and correspondence: Dr. Hideya Yamamoto, Department of Cardiovascular Medicine, Graduate School of Biomedical Sciences, Hiroshima University, 1-2-3 Kasumi Minami-ku, Hiroshima 734-8551, Japan. *E-mail:* [illegible].

1. Hausleiter J, Meyer T, Hadamitzky M, et al. Prevalence of noncalcified coronary plaques by 64-slice computed tomography in patients with an intermediate risk for significant coronary artery disease. J Am Coll Cardiol 2006;46:312–8.
2. Butler J, Shapiro M, Reiber J, et al. Extent and distribution of coronary artery disease: A comparative study of invasive versus noninvasive angiography with computed tomography. Am Heart J 2007;153:378–84.
3. Hoffmann U, Moselewski F, Nieman K, et al. Noninvasive assessment of plaque morphology and composition in culprit and stable lesions in acute coronary syndrome and stable lesions in stable angina by multidetector computed tomography. J Am Coll Cardiol 2006;47:1655–62.
4. Motoyama S, Kondo T, Sarai M, et al. Multislice computed tomographic characteristics of coronary lesions in acute coronary syndromes. J Am Coll Cardiol 2007;50:319–26.
5. Kitagawa T, Yamamoto H, Ohhashi N, et al. Comprehensive evaluation of noncalcified coronary plaque characteristics detected using 64-slice computed tomography in patients with proven or suspected coronary artery disease. Am Heart J 2007;154:1191–8.
6. Braunwald E, Antman EM, Beasley JW, et al. ACC/AHA 2002 guideline update for the management of patients with unstable angina and non–ST-segment elevation myocardial infarction-summary article: a report of the American College of Cardiology/American Heart Association Task Force on Practice Guidelines (Committee on the Management of Patients With Unstable Angina). J Am Coll Cardiol 2002;40:1366–74.

7. Achenbach S, Ropers D, Hoffmann U, et al. Assessment of coronary remodeling in stenotic and nonstenotic coronary atherosclerotic lesions by multidetector spiral computed tomography. J Am Coll Cardiol 2004;43:842–7.
8. Kajinami K, Seki H, Takekoshi N, et al. Coronary calcification and coronary atherosclerosis: site by site comparative morphologic study of electron beam computed tomography and coronary angiography. J Am Coll Cardiol 1997;29:1549–56.
9. Buffon A, Biasucci LM, Liuzzo G, et al. Widespread coronary inflammation in unstable angina. N Eng J Med 2002;347:5–12.
10. Rioufol G, Finet G, Ginon I, et al. Multiple atherosclerotic plaque rupture in acute coronary syndrome: a three-vessel intravascular ultrasound study. Circulation 2002;106:804–8.
11. Varnava AM, Mills PG, Davies MJ. Relationship between coronary artery remodeling and plaque vulnerability. Circulation 2002;105:939–43.
12. Chatzizisis YS, Coskun AU, Jonas M, Edelman ER, Feldman CL, Stone PH. Role of endothelial shear stress in the natural history of coronary atherosclerosis and vascular remodeling: molecular, cellular, and vascular behavior. J Am Coll Cardiol 2007;49:2379–93.
13. Hyafil F, Cornily JC, Feig JE, et al. Noninvasive detection of macrophages using a nanoparticulate contrast agent for computed tomography. Nat Med 2007;13:636–41.
14. Earls JP, Berman EL, Urban BA, et al. Prospectively gated transverse coronary CT angiography versus retrospectively gated helical technique: improved image quality and reduced radiation dose. Radiology 2008;246:742–53.

Key Words: acute coronary syndrome ▪ multidetector computed tomography ▪ noncalcified coronary plaque.

Endothelial Function and Oxidative Stress in Cardiovascular Diseases

Yukihito Higashi, MD; Kensuke Noma, MD;
Masao Yoshizumi, MD; Yasuki Kihara, MD*

The vascular endothelium is involved in the release of various vasodilators, including nitric oxide (NO), prostacyclin and endothelium-derived hyperpolarizing factor, as well as vasoconstrictors. NO plays an important role in the regulation of vascular tone, inhibition of platelet aggregation, and suppression of smooth muscle cell proliferation. Endothelial dysfunction is the initial step in the pathogenesis of atherosclerosis. Cardiovascular diseases are associated with endothelial dysfunction. It is well known that the grade of endothelial function is a predictor of cardiovascular outcomes. Oxidative stress plays an important role in the pathogenesis and development of cardiovascular diseases. Several mechanisms contribute to impairment of endothelial function. An imbalance of reduced production of NO or increased production of reactive oxygen species, mainly superoxide, may promote endothelial dysfunction. One mechanism by which endothelium-dependent vasodilation is impaired is an increase in oxidative stress that inactivates NO. This review focuses on recent findings and interaction between endothelial function and oxidative stress in cardiovascular diseases.

Key Words: Cardiovascular diseases; Endothelial function; Endothelium-derived factors; Oxidative stress

Various vasodilators, including nitric oxide (NO), prostacyclin, and endothelium-derived hyperpolarizing factor (EDHF), as well as vasoconstrictors, are released from the endothelium[1,2] NO plays an important role in the regulation of vascular tone, inhibition of platelet aggregation, and suppression of vascular smooth muscle cell proliferation[3,4] Impaired endothelium-dependent vasodilation has been found in the forearm, coronary, and renal vasculature of patients with hypertension[5–11] dyslipidemia[12,13] diabetes mellitus[14–16] and coronary artery diseases[17–21] Endothelial dysfunction is an early feature of both atherosclerosis and vascular diseases in humans[22] Improvement or augmentation of endothelial function will prevent the development of atherosclerosis, resulting in a reduction in cardiac events.

There are several possible mechanisms for impaired endothelial function in patients with cardiovascular diseases. Decreased NO bioavailability (decreased NO production and/or increased NO inactivation) induces endothelial dysfunction. A balance of endothelium-derived vasodilators, especially NO, and reactive oxygen species (ROS) modulates endothelial function. Therefore, an imbalance of NO and ROS, so-called oxidative stress, is involved in endothelial dysfunction through the inactivation of NO.

(Received November 26, 2008; revised manuscript received December 5, 2008; accepted December 14, 2008; released online February 4, 2009)

*Departments of Cardiovascular Physiology and Medicine, *Cardiovascular Medicine, Hiroshima University Graduate School of Biomedical Sciences, Hiroshima, Japan*
Mailing address: Yukihito Higashi, MD, Department of Cardiovascular Physiology and Medicine, Hiroshima University Graduate School of Biomedical Sciences, 1-2-3 Kasumi, Minami-ku, Hiroshima 734-8551, Japan. E-mail: yhigashi@hiroshima-u.ac.jp

Oxidative Stress in Cardiovascular Diseases

ROS are produced by various oxidase enzymes, including nicotinamide-adenine dinucleotide phosphate (NADPH) oxidase, xanthine oxidase, uncoupled endothelial NO synthase (eNOS), cyclooxygenase, glucose oxidase, and lipooxygenase, and mitochondrial electron transport (**Fig 1**). ROS include superoxide anion (O_2^-), hydrogen peroxide (H_2O_2), hydroxyl radical (OH), hypochlorous acid (HOCl), NO, and peroxynitrite ($ONOO^-$). O_2^-, OH, and NO are classified as free radicals that have unpaired electrons and potent oxidation ability. H_2O_2, HOCl, and $ONOO^-$ are classified as non-free radicals that also have oxidation ability. The sources of ROS are a variety of cell types, including vascular smooth muscle cells (VSMCs), endothelial cells and mononuclear cells. The antioxidant enzyme superoxide dismutase (SOD) has been identified as 3 enzymatic types: Cu/Zn SOD, Mn SOD, and extracellular SOD. SOD rapidly dismutates O_2^- to H_2O_2, then H_2O_2 is eliminated by glutathione peroxidase (GPx) and catalase to water.

Several lines of evidence demonstrate that oxidative stress plays an important role in the pathogenesis and development of cardiovascular diseases, including hypertension, dyslipidemia, diabetes mellitus, atherosclerosis, myocardial infraction, angina pectoris, and heart failure[23–26] The susceptibility of vascular cells to oxidative stress is a function of the overall balance between the degree of oxidative stress and the antioxidant defense capability. Protective antioxidant mechanisms are complex and multifactorial. Antioxidant defense systems, such as SOD, GPx and catalase, scavenge ROS in the vasculature, resulting in inhibition of NO degradation. Although SOD rapidly converts O_2^- to H_2O_2, H_2O_2 per se is involved as an intracellular second messenger in vascular remodeling, inflammation, apoptosis, and growth of VSMCs[27] Oxidative stress induces cell proliferation, hypertrophy, apoptosis and inflammation through activation of various signaling cascades and redox-

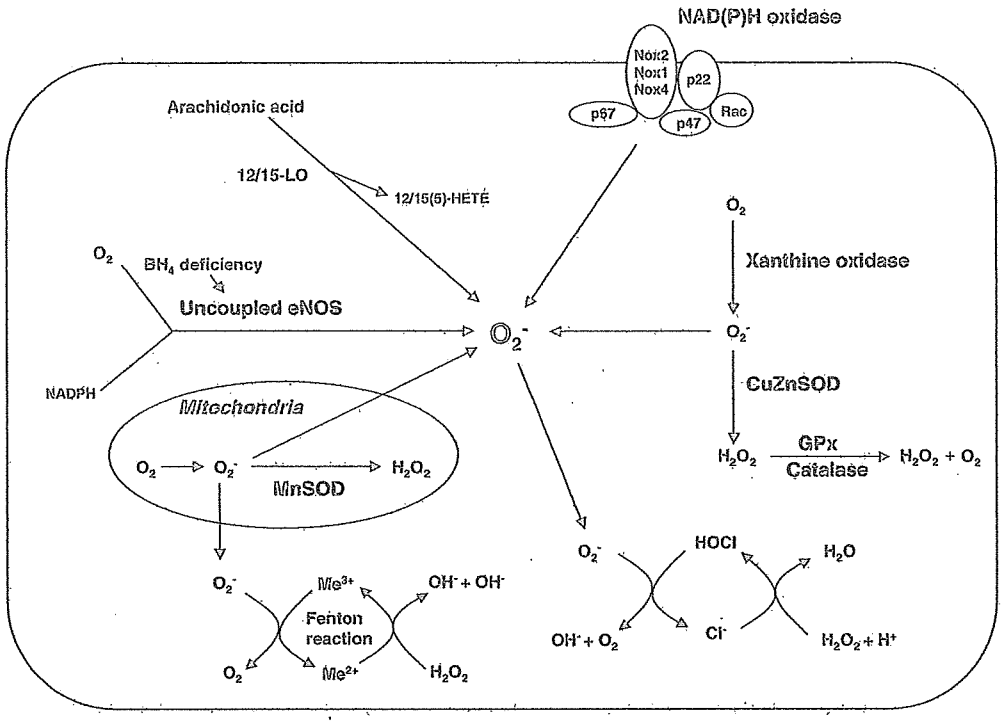

Fig 1. Activated NADH/NADPH oxidase-related ROS generation and ROS degradation system in the vasculature. NADPH, nicotinamide adenine dinucleotide phosphate; ROS, reactive oxygen species; SOD, superoxide dismutase; NO, nitric oxide; GPx, glutathione peroxidase; eNOS, endothelial NO synthase.

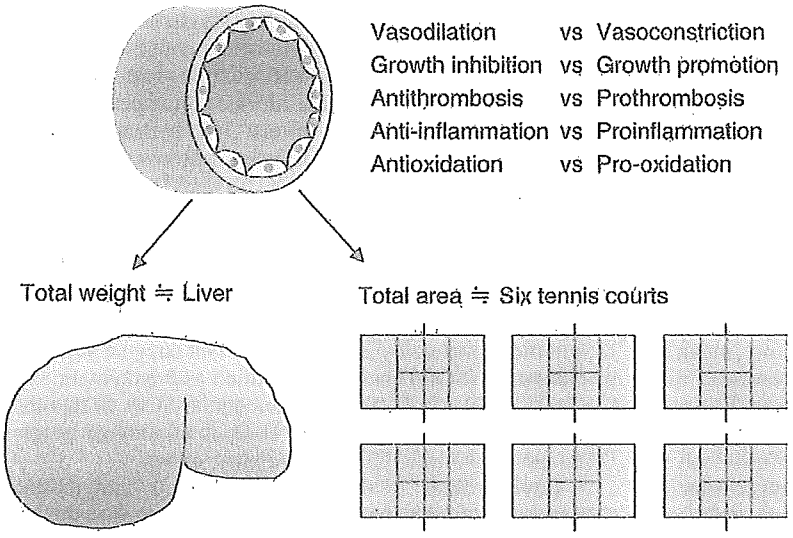

Fig 2. Structure and function of endothelial cells.

sensitive transcriptional factors. Excess ROS, especially free radicals, oxidize various molecules. Lipid peroxidation and protein oxidation induce overexpression of redox genes, intracellular calcium overload, and DNA fragmentation, resulting in damage to VSMCs, endothelial cells or myocardial cells. A vicious cycle of oxidative stress and oxidative stress-induced atherosclerosis leads to the development of atherosclerosis.

Endothelial Function in Cardiovascular Diseases

It had been thought until 1981 that the vascular endothelium functioned as a wall separating the blood vessel and the inside cavity. If the endothelium of the whole body could be collected, its total weight would be equal to that of the liver, and its total area would be equal to that of 6 tennis courts. Endothelial cells secrete various vasoactive agents, such as the vasodilators NO, prostacyclin and EDHF, and the vasoconstrictors endothelin-1, angiotensin II (AngII), and thromboxane A_2.[1–4] Thus, the vascular endothelium might be the biggest endocrine organ in the human body. A healthy endothelium maintains vascular tone and structure by regulating the balance between vasodilation and vasoconstriction, growth inhibition and growth promotion, antithrombosis and prothrombosis, anti-inflammation and pro-

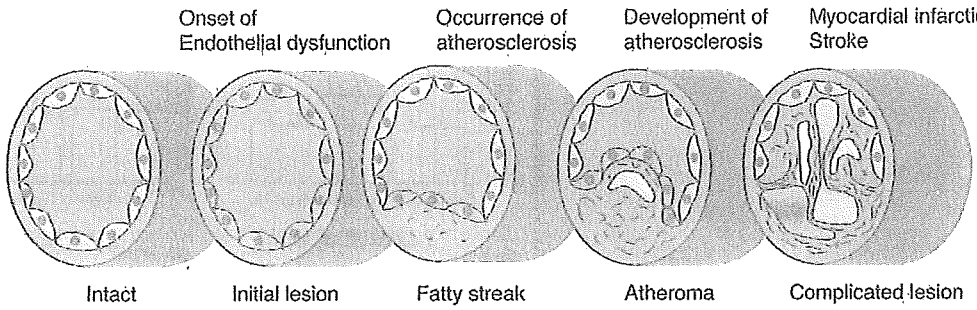

Fig3. From endothelial dysfunction to cardiovascular complications: progression of atherosclerosis in cardiovascular diseases.

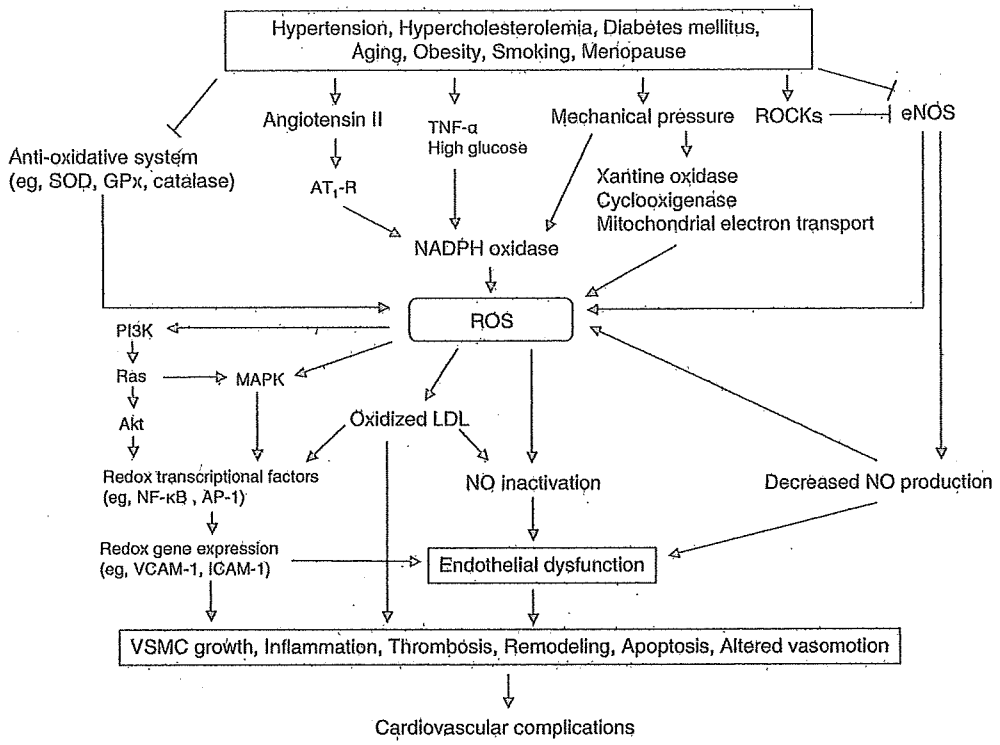

Fig4. Mechanisms by which ROS induce endothelial dysfunction. NO, nitric oxide (NO); ROCK, Rho-associated kinase; SOD, superoxide dismutase; NADH/NADPH, nicotinamide adenine dinucleotide phosphate; ROS, reactive oxygen species; HSP, heat shock protein; HIF-1, hypoxia-induced factor-1; VEGF, vascular endothelial growth factor; eNOS, endothelial NO synthase; PI3K, phosphatidyl-inositol-3-kinase; MAPK, mitogen-activated protein kinase; NF-κB, nuclear factor κB; AP-1, plasminogen activator inhibitor-1; VCAM-1, vascular cell adhesion molecule-1; ICAM-1, intracellular adhesion molecule-1; VSMC, vascular smooth muscle cell.

inflammation, and also antioxidation and pro-oxidation (**Fig2**).[1–4]

Endothelial dysfunction is the initial step in the pathogenesis of atherosclerosis (**Fig3**).[22] Several investigators have shown that impaired endothelium-dependent vasodilation is found in the forearm, coronary, and renal vasculature in patients with cardiovascular diseases.[5–21] Perticone et al evaluated cardiac outcome in patients with untreated essential hypertension characterized by 3 tertiles of acetylcholine-induced vasodilation, and found that patients with the lowest tertile of acetylcholine-induced vasodilation had a significantly higher event ratio than did the patients with a moderate or high tertile.[28] In patients with coronary artery diseases, severe coronary endothelial dysfunction is associated with increased cardiovascular events.[29] Schachinger et al demonstrated a link between coronary endothelial dysfunction and subsequent cardiovascular events in patients with coronary artery diseases.[30] Acetylcholine-induced vasodilation and flow-meditated vasodilation are also useful for predicting cardiovascular events in such patients.[23–25] Also in patients with peripheral arterial disease, conduit artery endothelial dysfunction assessed by flow-meditated vasodilation independently predicts long-term cardiac outcome.[26] Those clinical studies have shown that endothelial function can be an independent predictor of cardiovascular events.[30,31]

From a clinical perspective, it is important to select an appropriate intervention that will be effective in improving endothelial function in patients with cardiovascular diseases. Indeed, several interventions, including pharmacological therapy, administration of antihypertensive agents such as

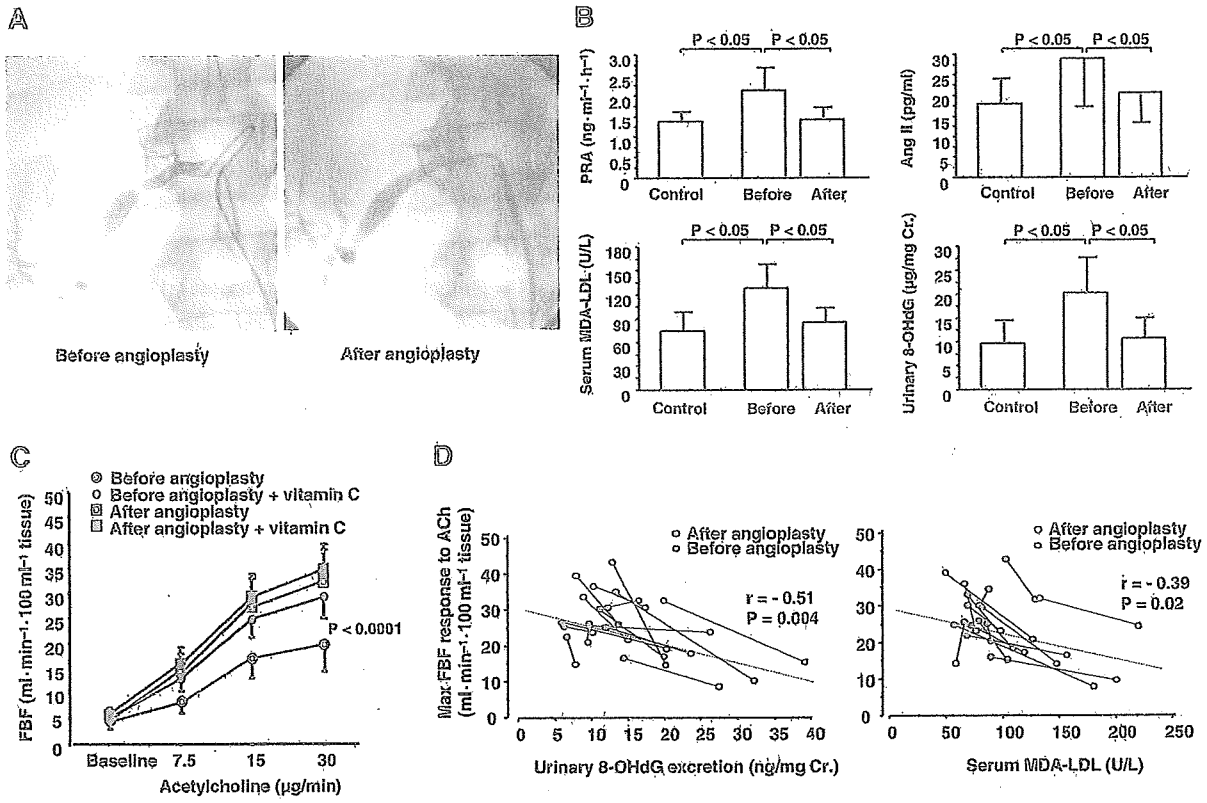

Fig 5. Endothelial function and oxidative stress in patients with renovascular hypertension. (A) Angiography before and after angioplasty. (B) Circulating renin and AngII levels and oxidative stress markers before and after angioplasty. (C) Effects of concomitant administration of the antioxidant vitamin C on the forearm blood flow response to acetylcholine administration before and after angioplasty. (D) Relationship between acetylcholine-induced vasodilation and oxidative stress. Modified from Ref. 66 with permission. Copyright ©2002 Massachusetts Medical Society. All rights reserved. AngII, angiotensin II.

angiotensin-converting enzyme inhibitors and AngII type I receptor blockers;[32–35] statins;[36] and thiazolidinedione derivatives;[37] supplementation therapy, such as administration of a substrate of NO L-arginine;[38] estrogen replacement;[39] administration of a cofactor of NO tetrahydrobiopterine;[40] treatment with antioxidant vitamins such as vitamin C;[41] and lifestyle modifications such as aerobic exercise;[7,42,43] body weight reduction;[44] and sodium restriction;[45] have been shown to improve endothelial function and prevent cardiovascular complications. These findings suggest that endothelial dysfunction in patients with cardiovascular diseases is reversible.

Several investigators have reported possible mechanisms of the impairment of endothelial function in cardiovascular diseases, including abnormalities of shear stress, increased amounts of the endogenous eNOS inhibitor asymmetrical dimethylarginine, increased amounts of vasoconstrictors such as AngII, endothelin-1 and norepinephrine, and inactivation of NO by ROS.[46,47] Growing evidence reveals an interaction between oxidative stress and endothelial function (Fig 4). Enhanced production of ROS and an attenuated antioxidant system would contribute to endothelial dysfunction in cardiovascular diseases.

Decrease in NO Bioavailability

Endothelial dysfunction has been shown to be associated with an increase in ROS in atherosclerotic animal models and human subjects with atherosclerosis.[46] The concentrations of antioxidant scavengers, such as SOD, GPx catalase, and vitamins C and E, are decreased in patients with atherosclerosis.[48] NADH/NADPH oxidase, which is a major source of production of ROS in vessel walls, is activated in experimental models of atherosclerosis.[49,50] It has also been shown that ascorbic acid (vitamin C) restores impaired endothelium-dependent vasodilation in patients with essential hypertension, dyslipidemia, and coronary artery diseases.[13,17,51] Enhanced NO inactivation caused by excess ROS production, rather than decreased NO production, may play an important role in the impairment of endothelium-dependent vasodilation. These findings suggest that a decrease in NO inactivation induces an improvement in the endothelial dysfunction in patients with cardiovascular diseases.

eNOS

The serine/threonine kinase Akt protooncogene is 1 of the major regulators of various cellular processes and mediates the activation of eNOS, resulting in increased NO production from endothelial cells.[52] Fulton et al[53] showed that Akt activates eNOS enzyme activity by phosphorylation of eNOS, independently of an increase in intracellular free calcium concentration, leading to an increase in NO production from endothelial cells. The phosphatidyl-inositol-3-kinase (PI3K)/Akt pathway, which causes intracellular calcium-independent eNOS phosphorylation and activation, is involved in eNOS activation, in addition to a calcium-

dependent mechanism.

Under pathologic conditions, the PI3K/Akt pathway is diminished, resulting in decreased levels of eNOS gene expression and enzymatic activity. Andreozzi et al demonstrated that AngII enhanced Ser312 and Ser616 phosphorylation of insulin receptor substrate-1 through stimulation of c-Jun N-terminal kinase and extracellular signal-regulated kinase 1/2 activity in human umbilical vein endothelial cells, and that it impaired insulin-mediated vasodilation through inactivation of the insulin receptor substrate-1/PI3K/Akt/eNOS pathway.[54] Indeed, chronic inhibition of the renin-angiotensin system (RAS) improves endothelial function by either increasing NO production or by activating eNOS-related NO production.[55] In addition, chronic inhibition of the RAS has been shown to lead to functional and histological alterations of the vascular endothelium, resulting in enhanced vascular structure and function.[55]

eNOS per se produces ROS rather than NO under the condition of eNOS uncoupling through a deficiency of tetrahydrobiopterin (BH_4), an essential cofactor for eNOS, or oxidation of BH_4. Degradation of BH_4 by ROS, including $ONOO^-$, O_2^- and H_2O_2, is associated with downregulation of eNOS.[56] In addition, it has been demonstrated that supplementation of BH_4 improves endothelial function in vivo and in vitro, and in smokers and patients with hypertension, hypercholesterolemia or chronic heart failure.[57–60] Recently, we also showed that the grade of oxidative stress correlates with a deficiency of BH_4, and that supplementation with BH_4 augmented endothelium-dependent vasodilation in the brachial arteries of elderly subjects.[61] These findings suggest that BH_4 deficiency and decreased eNOS activity cause endothelial dysfunction in atherosclerotic patients through an increase in oxidative stress.

NADH/NADPH Oxidase

NADH/NADPH oxidase is the most important source of ROS in the vasculature.[62] NADH/NADPH oxidase is a multi-subunit complex composed of cytosolic components, such as $p47^{phox}$, $p67^{phox}$ and Rac 1, and membrane-spanning components, such as $p22^{phox}$ and $gp91^{phox}$ or another NOx homolog. The production of ROS by activated NADH/NADPH oxidase is mediated by several pathways.[63] AngII-induced NADH/NADPH oxidase activation is 1 of the major sources of ROS in atherosclerosis.[62–65] The activated NADH/NADPH oxidase-related ROS generation and ROS degradation pathway is shown in **Fig 1**. In the aorta of spontaneously hypertensive rats, endothelial dysfunction is caused by an excess of ROS rather than a decrease in NO production and is associated with both upregulation of $p22^{phox}$ mRNA expression and increased activity of NADH/NADPH oxidase.[63] Upregulation of $p22^{phox}$ mRNA expression is a key component of AngII-induced NADH/NADPH oxidase activation, and increased expression levels of other components also play an important role in this oxidase under pathological conditions.[64,65] Increased mRNA expression levels of $p47^{phox}$, $p67^{phox}$, $p22^{phox}$ and NOx2 have been found in the internal mammary arteries of patients with coronary artery diseases and in those with diabetes mellitus. RAS inhibitors prevent the increase in the mRNA expression levels of $p22^{phox}$ and NOx2 in AngII-induced hypertensive rats and reduce ROS generation, and the AT_2 receptor blockade accentuated the changes in $p22^{phox}$ and NOx2 and increased $p67^{phox}$. RAS inhibition improves endothelial function in various animal models through decreased NADH/NADPH oxidase activity.[63] It is thought that inactivation of NADH/NADPH oxidase may contribute to the improvement in endothelial dysfunction in patients with atherosclerosis. Recently, we also found that inactivation of the RAS, particularly AngII, by successful renal angioplasty may decrease oxidative stress, resulting in improved endothelium-dependent vasodilation in patients with renovascular hypertension, who are ideal subjects for determining how endothelial function is affected by excess AngII and AngII-related increase in oxidative stress (**Fig 5**).[66] These findings suggest that the role of the RAS in the pathogenesis of atherosclerosis may be related, at least in part, to AngII-induced production of ROS in vascular cells.

Antioxidant System

Protective antioxidant mechanisms are complex and multifactorial. The antioxidant defense system, such as SOD, GPx and catalase, scavenges ROS in the vasculature, resulting in inhibition of NO degradation (**Fig 1**). The susceptibility of vascular cells to oxidative stress is a function of the overall balance between the degree of oxidative stress and the antioxidant defense capability. The antioxidant enzyme SOD rapidly dismutates O_2^- to H_2O_2. SOD has been identified as 3 enzymatic types: Cu/Zn SOD, Mn SOD, and extracellular SOD. Destruction of the antioxidant system, including decreased antioxidant enzyme activity and ROS scavenging ability, may contribute to oxidative stress in patients with atherosclerosis. Various interventions, such as administration of antioxidant vitamins and antihypertensive agents and exercise training, have been shown to enhance the protein levels and enzymatic activities of SOD, such as Cu/Zn SOD and Mn SOD, in the vascular endothelium and smooth muscle cells of the aorta in experimental animal models.[67,68] It has been reported that approximately 50% of the total SOD in the human vasculature is extracellular.[69] Fukai et al demonstrated that exercise increased eNOS and extracellular SOD protein levels in wild-type mice, but had no effect on extracellular SOD protein levels in eNOS-knockout mice and that the effect of endothelium-derived NO on extracellular SOD protein level is mediated by the cGMP/protein kinase G-dependent pathway.[70] Hornig et al have shown that extracellular SOD contributes to the improvement in endothelial function by treatment with a RAS inhibitor in patients with coronary artery diseases.[71] Interestingly, extracellular SOD activity determined after its release from the endothelium by a heparin bolus injection was increased after treatment with losartan and was associated with an increase in flow-mediated vasodilation. These findings suggest that activation of extracellular SOD improves endothelial function, probably by increased NO bioavailability, in patients with coronary artery diseases.

Although SOD rapidly converts O_2^- to H_2O_2, H_2O_2 per se is involved as an intracellular second messenger in vascular remodeling, inflammation, apoptosis, and growth of VSMCs. Hydrogen peroxide is eliminated by GPx and catalase to H_2O. It has been shown that a physiological level of shear stress upregulates GPx mRNA levels and GPx enzymatic activity in cultured bovine aortic endothelial cells.[72] The upregulation of Cu/Zn SOD, Mn SOD, GPx and catalase, apart from extracellular SOD induced by appropriate interventions, may improve endothelial function through the inhibition of NO degradation with a decrease in ROS.

Rho-Associated Kinases (ROCKs)

The family of ROCKs, which are small GTPase Rho effectors, mediate various cellular physiologic functions

such as cell proliferation, migration, adhesion, apoptosis and contraction, all of which may be involved in the pathogenesis of atherosclerosis[73–75] ROCKs consist of 2 isoforms, ROCK1 and ROCK2, and have been found to be the immediate downstream targets of RhoA[76,77] The RhoA/ROCK pathway has been shown to be involved in the formation of atherosclerotic lesions, vasoconstriction and myocardial hypertrophy, and to be activated in patients with hypertension and in those with coronary artery disease[78–83] Sauzeau et al have shown that NO also inhibits RhoA translocation from the cytosol to the membrane in VSMCs[84] In addition, previous studies using ROCK inhibitors, such as fasudil or Y-27632, have suggested that ROCKs may play an important role in the pathogenesis of cardiovascular disease[74,78,80] These experimental and clinical studies have shown that ROCKs are an important therapeutic target for cardiovascular diseases[85,86] Previous studies have shown that activation of the RhoA/ROCK pathway impairs NO bioavailability through inhibition of eNOS mRNA stability and eNOS protein phosphorylation at Ser1177 via the PI3K/Akt pathway[78,87] We previously reported that intra-arterial infusion of the ROCK inhibitor fasudil improved endothelial function in smokers[88] Several investigators have shown an interaction between the RhoA/ROCK pathway and ROS[89,90] Indeed, ROS induced by hyperglycemia enhance ROCK activity, leading to atherothrombogenesis through increased expression of plasminogen activator inhibitor-1 in vascular endothelial cells[91] It is well known that cigarette smoking decreases NO bioavailability through the production of ROS. Several investigators, including us, have demonstrated that there is a possible association of ROCK activity with oxidative stress and that smoking enhances the activation of ROCKs in VSMCs in vivo and in vitro[89,92] Taken together, the findings indicate an interaction between ROCK activity, endogenous NO, and oxidative stress.

Conclusions

Increased production of ROS impairs endothelial function in humans. One mechanism by which endothelial function is impaired is increased oxidative stress, which inactivates NO. An imbalance of reduced production of NO and increased production of ROS may be involved in impaired endothelium-dependent vasodilation in patients with cardiovascular diseases. It is thought that a vicious cycle of endothelial dysfunction and oxidative stress leads to development of atherosclerosis. In the clinical setting, it is important to select appropriate interventions for both endothelial function and oxidative stress, and it is expected such interventions will greatly improve clinical outcomes. Future study in a large clinical trial or cohort study is needed to determine the roles of endothelial function and oxidative stress in cardiovascular outcomes.

Acknowledgments

The authors thank Megumi Wakisaka and Satoko Michiyama for their excellent secretarial assistance.

Disclosures

This study was supported in part by a Grant-in-Aid for Scientific Research from the Ministry of Education, Culture, Sports, Science and Technology of Japan (1559075100 and 1859081500).

Conflict of interest is none.

References

1. Lüscher TF. Imbalance of endothelium-derived relaxing and contracting factors. *Am J Hypertens* 1990; **3:** 317–330.
2. Vane JR, Anggard EE, Botting RM. Regulatory functions of the vascular endothelium. *N Engl J Med* 1990; **323:** 27–36.
3. Vallance P, Collier J, Moncada S. Effects of endothelium-derived nitric oxide on peripheral arteriolar tone in man. *Lancet* 1989; **2:** 997–1000.
4. Vanhoutte PM. Endothelium and control of vascular function: State of the art lecture. *Hypertension* 1989; **13:** 658–667.
5. Panza JA, Quyyumi AA, Brush JE Jr, Epstein SE. Abnormal endothelium-dependent vascular relaxation in patients with essential hypertension. *N Engl J Med* 1990; **323:** 22–27.
6. Linder L, Kiowski W, Buhler FR, Lüscher TF. Indirect evidence for release of endothelium-derived relaxing factor in human forearm circulation in vivo: Blunted response in essential hypertension. *Circulation* 1990; **81:** 1762–1767.
7. Higashi Y, Sasaki S, Kurisu S, Yoshimizu A, Sasaki N, Matsuura H, et al. Regular aerobic exercise augments endothelium-dependent vascular relaxation in normotensive as well as hypertensive subjects: Role of endothelium-derived nitric oxide. *Circulation* 1999; **100:** 1194–1202.
8. Treasure CB, Klein JL, Vita JA, Manoukian SV, Renwick GH, Selwyn AP, et al. Hypertension and left ventricular hypertrophy are associated with impaired endothelium-mediated relaxation in human coronary resistance vessels. *Circulation* 1993; **87:** 86–93.
9. Egashira K, Suzuki S, Hirooka Y, Kai H, Sugimachi M, Imaizumi T, et al. Impaired endothelium-dependent vasodilation in large epicardial and resistance coronary arteries in patients with essential hypertension: Different responses to acetylcholine and substance P. *Hypertension* 1995; **25:** 201–206.
10. Raij L. Nitric oxide and the kidney. *Circulation* 1993; **87**(Suppl V): V-26–V-29.
11. Higashi Y, Oshima T, Ozono R, Watanabe M, Matsuura H, Kajiyama G. Effects of L-arginine infusion on renal hemodynamics in patients with mild essential hypertension. *Hypertension* 1995; **25:** 898–902.
12. Creager MA, Cooke JP, Mendelsohn ME, Gallagher SJ, Coleman SM, Loscalzo J, et al. Impaired vasodilation of forearm resistance vessels in hypercholesterolemic humans. *J Clin Invest* 1990; **86:** 228–234.
13. Gilligan DM, Sack MN, Guetta V, Casino PR, Quyyumi AA, Rader DJ, et al. Effect of antioxidant vitamins on low density lipoprotein oxidation and impaired endothelium-dependent vasodilation in patients with hypercholesterolemia. *J Am Coll Cardiol* 1994; **24:** 1611–1617.
14. Ting HH, Timimi FK, Boles KS, Creager SJ, Ganz P, Creager MA. Vitamin C improves endothelium-dependent vasodilation in patients with non-insulin-dependent diabetes mellitus. *J Clin Invest* 1996; **97:** 22–28.
15. McVeigh GE, Brennan GM, Johnston GD, McDermott BJ, McGrath LT, Henry WR, et al. Impaired endothelium-dependent and independent vasodilation in patients with type 2 (non-insulin-dependent) diabetes mellitus. *Diabetologia* 1992; **35:** 771–776.
16. Clarkson P, Celermajer DS, Donald AE, Sampson M, Sorensen KE, Adams M, et al. Impaired vascular reactivity in insulin-dependent diabetes mellitus is related to disease duration and low density lipoprotein cholesterol levels. *J Am Coll Cardiol* 1996; **28:** 573–579.
17. Levine GN, Frei B, Koulouris SN, Gerhard MD, Keaney JF Jr, Vita JA. Ascorbic acid reverses endothelial vasomotor dysfunction in patients with coronary artery disease. *Circulation* 1996; **93:** 1107–1113.
18. Zeiher AM, Drexler H, Saurbier B, Just H. Endothelium-mediated coronary blood flow modulation in humans: Effects of age, atherosclerosis, hypercholesterolemia, and hypertension. *J Clin Invest* 1993; **92:** 652–662.
19. Soga J, Nishioka K, Nakamura S, Umemura T, Jitsuiki D, Hidaka T, et al. Measurement of flow-mediated vasodilation of the brachial artery: A comparison of measurements in the sitting and supine positions. *Circ J* 2007; **71:** 736–740.
20. Treasure CB, Klein JL, Weintraub WS, Talley JD, Stillabower ME, Kosinski AS, et al. Beneficial effects of cholesterol-lowering therapy on the coronary endothelium in patients with coronary artery disease. *N Engl J Med* 1995; **332:** 481–467.
21. Hambrecht R, Wolf A, Gielen S, Linke A, Hofer J, Erbs S, et al. Effect of exercise on coronary endothelial function in patients with coronary artery disease. *N Engl J Med* 2000; **342:** 454–460.
22. Ross R. Atherosclerosis: An inflammatory disease. *N Engl J Med* 1999; **340:** 115–126.
23. Schachinger V, Britten MB, Zeiher AM. Prognostic impact of coronary vasodilator dysfunction on adverse long-term outcome of coro-

nary heart disease. *Circulation* 2000; **101:** 1899–1906.
24. Heitzer T, Schlinzig T, Krohn K, Meinertz T, Munzel T. Endothelial dysfunction, oxidative stress, and risk of cardiovascular events in patients with coronary artery disease. *Circulation* 2001; **104:** 2673–2678.
25. Neunteufl T, Heher S, Katzenschlager R, Wolfl G, Kostner K, Maurer G, et al. Late prognostic value of flow-mediated dilation in the brachial artery of patients with chest pain. *Am J Cardiol* 2000; **86:** 207–210.
26. Gokce N, Keaney JF Jr, Hunter LM, Watkins MT, Menzoian JO, Vita JA. Risk stratification for postoperative cardiovascular events via noninvasive assessment of endothelial function: A prospective study. *Circulation* 2002; **105:** 1567–1572.
27. Faraci FM, Didion SP. Vascular protection: Superoxide dismutase isoforms in the vessel wall. *Arterioscler Thromb Vasc Biol* 2004; **24:** 1367–1373.
28. Perticone F, Ceravolo R, Pujia A, Ventura G, Iacopino S, Scozzafava A, et al. Prognostic significance of endothelial dysfunction in hypertensive patients. *Circulation* 2001; **104:** 191–196.
29. Suwaidi JA, Hamasaki S, Higano ST, Nishimura RA, Holmes DR Jr, Lerman A. Long-term follow-up of patients with mild coronary artery disease and endothelial dysfunction. *Circulation* 2000; **101:** 948–954.
30. Widlansky ME, Gokce N, Keaney JF Jr, Vita JA. The clinical implications of endothelial dysfunction. *J Am Coll Cardiol* 2003; **42:** 1149–1160.
31. Landmesser U, Hornig B, Drexler H. Endothelial function: A critical determinant in atherosclerosis? *Circulation* 2004; **109**(Suppl 1): II-27–II-33.
32. Hirooka Y, Imaizumi T, Masaki H, Ando S, Harada S, Momohara M, et al. Captopril improves impaired endothelium-dependent vasodilation in hypertensive patients. *Hypertension* 1992; **20:** 175–180.
33. Schiffrin EL, Deng LY. Comparison of effects of angiotensin I-converting enzyme inhibition and β-blockade for 2 years on function of small arteries from hypertensive patients. *Hypertension* 1995; **25:** 699–703.
34. Higashi Y, Sasaki S, Nakagawa K, Kurisu S, Yoshimizu A, Matsuura H, et al. A comparison of angiotensin-converting enzyme inhibitors, calcium antagonists, beta-blockers, diuretics on reactive hyperemia in patients with essential hypertension: A multicenter study. *J Am Coll Cardiol* 2000; **35:** 284–291.
35. Ghiadoni L, Virdis A, Magagna A, Taddei S, Salvetti A. Effect of the angiotensin II type 1 receptor blocker candesartan on endothelial function in patients with essential hypertension. *Hypertension* 2000; **35:** 501–506.
36. Wolfrum S, Jensen KS, Liao JK. Endothelium-dependent effects of statins. *Arterioscler Thromb Vasc Biol* 2003; **23:** 729–736.
37. Martens FM, Rabelink TJ, op 't Roodt J, de Koning EJ, Visseren FL. TNF-alpha induces endothelial dysfunction in diabetic adults, an effect reversible by the PPAR-gamma agonist pioglitazone. *Eur Heart J* 2006; **27:** 1605–1609.
38. Higashi Y, Oshima T, Ozono R, Watanabe M, Matsuura H, Kajiyama G. Effects of L-arginine infusion on renal hemodynamics in patients with mild essential hypertension. *Hypertension* 1995; **25:** 898–902.
39. Sanada M, Higashi Y, Sasaki S, Nakagawa K, Kodama I, Tsuda M, et al. Relationship between the angiotensin-converting enzym genotype and forearm vasodilator response to estrogen replacement therapy in postmenopausal. *J Am Coll Cardiol* 2001; **37:** 1529–1535.
40. Higashi Y, Sasaki S, Nakagawa K, Fukuda Y, Matsuura H, Oshima T, et al. Tetrahydrobiopterin improves impaired endothelium-dependent vasodilation in patients with essential hypertension. *Am J Hypertens* 2002; **15:** 326–332.
41. Takeshita Y, Katsuki Y, Katsuda Y, Kai H, Saito Y, Arima K, et al. Vitamin C reversed malfunction of peripheral blood-derived mononuclear cells in smokers through antioxidant properties. *Circ J* 2008; **72:** 654–659.
42. Higashi Y, Sasaki S, Sasaki N, Nakagawa K, Ueda T, Yoshimizu A, et al. Daily aerobic exercise improves reactive hyperemia in patients with essential hypertension. *Hypertension* 1999; **33:** 591–597.
43. Goto C, Higashi Y, Kimura M, Noma K, Hara K, Nakagawa K, et al. The effect of different intensities of exercise on endothelium-dependent vasodilation in humans: Role of endothelium-dependent nitric oxide and oxidative stress. *Circulation* 2003; **108:** 530–535.
44. Sasaki S, Higashi Y, Nakagawa K, Kimura M, Noma K, Sasaki S, et al. A low-calorie diet improves endothelium-dependent vasodilation in obese patients with essential hypertension. *Am J Hypertens* 2002; **15:** 302–309.
45. Bragulat E, de la Sierra A, Antonio MT, Coca A. Endothelial dysfunction in salt-sensitive essential hypertension. *Hypertension* 2001; **37:** 444–448.
46. Cai H, Harrison DG. Endothelial dysfunction in cardiovascular diseases: The role of oxidant stress. *Circ Res* 2000; **87:** 840–844.
47. Delles C, Schneider MP, John S, Gekle M, Schmieder RE. Angiotensin converting enzyme inhibition and angiotensin II AT1-receptor blockade reduce the levels of asymmetrical N(G), N(G)-dimethylarginine in human essential hypertension. *Am J Hypertens* 2002; **15:** 590–593.
48. Irani K. Oxidant signaling in vascular cell growth, death and survival: A review of the roles of reactive oxygen species in smooth muscle and endothelial cell mitogenic and apoptotic signaling. *Circ Res* 2000; **87:** 179–183.
49. Rajagopalan S, Kurz S, Munzel T, Tarpey M, Freeman BA, Griendling KK, et al. Angiotensin II-mediated hypertension in the rat increases vascular superoxide production via membrane NADH/NADPH oxidase activation. *J Clin Invest* 1996; **97:** 1916–1923.
50. Hegde LG, Srivastava P, Kumari R, Dikshit M. Alterations in the vasoreactivity of hypertensive rat aortic rings: Role of nitric oxide and superoxide radicals. *Clin Exp Hypertens* 1998; **20:** 885–901.
51. Hornig B. Vitamins, antioxidants and endothelial function in coronary artery disease. *Cardiovasc Drugs Ther* 2002; **16:** 401–409.
52. Dimmeler S, Fleming I, Fisslthaler B, Hermann C, Busse R, Zeiher AM. Activation of nitric oxide synthase in endothelial cells by Akt-dependent phosphorylation. *Nature* 1999; **399:** 601–605.
53. Fulton D, Gratton JP, McCabe TJ, Fontana J, Fujio Y, Walsh K, et al. Regulation of endothelium-derived nitric oxide production by the protein kinase Akt. *Nature* 1999; **399:** 597–601.
54. Andreozzi F, Laratta E, Sciacqua A, Perticone F, Sesti G. Angiotensin II impairs the insulin signaling pathway promoting production of nitric oxide by inducing phosphorylation of insulin receptor substrate-1 on Ser312 and Ser616 in human umbilical vein endothelial cells. *Circ Res* 2004; **94:** 1211–1218.
55. Dijhorst-Oei LT, Stores ES, Koomans HA, Rabelink TJ. Acute simultaneous stimulation of nitric oxide and oxygen radicals by angiotensin II in humans in vivo. *J Cardiovasc Pharmacol* 1999; **33:** 420–424.
56. Kuzkaya N, Weissmann N, Harrison DG, Dikalov S. Interactions of peroxynitrite, tetrahydrobiopterin, ascorbic acid, and thiols: Implications for uncoupling endothelial nitric-oxide synthase. *J Biol Chem* 2003; **278:** 22546–22554.
57. Masano T, Kawashima S, Toh R, Satomi-Kobayashi S, Shinohara M, Takaya T, et al. Beneficial effects of exogenous tetrahydrobiopterin on left ventricular remodeling after myocardial infarction in rats: The possible role of oxidative stress caused by uncoupled endothelial nitric oxide synthase. *Circ J* 2008; **72:** 1512–1519.
58. Heitzer T, Brockhoff C, Mayer B, Warnholtz A, Mollnau H, Henne S, et al. Tetrahydrobiopterin improves endothelium-dependent vasodilation in chronic smokers: Evidence for a dysfunctional nitric oxide synthase. *Circ Res* 2000; **86:** E36–E41.
59. Stoes E, Kastelein J, Cosentino F, Erkelens W, Wever R, Koomans H, et al. Tetrahydrobiopterin restores endothelial function in hypercholesterolemia. *J Clin Invest* 1997; **99:** 41–46.
60. Setoguchi S, Hirooka Y, Eshima K, Shimokawa H, Takeshita A. Tetrahydrobiopterin improves impaired endothelium-dependent forearm vasodilation in patients with heart failure. *J Cardiovasc Pharmacol* 2002; **39:** 363–368.
61. Higashi Y, Sasaki S, Nakagawa K, Kimura M, Noma K, Hara K, et al. Tetrahydrobiopterin improves aging-related impairment of endothelium-dependent vasodilation through increase in nitric oxide production and decrease in reactive oxygen species. *Atherosclerosis* 2006; **186:** 390–395.
62. Dzau VJ. Tissue angiotensin and pathobiology of vascular disease: A unifying hypothesis [Theodore Cooper Lecture]. *Hypertension* 2001; **37:** 1047–1052.
63. Zalba G, Beaumont FJ, San Jose G, Fortuno A, Fortuno MA, Etayo JC, et al. Vascular NADH/NADPH oxidase is involved in enhanced superoxide production in spontaneously hypertensive rats. *Hypertension* 2000; **35:** 1055–1061.
64. Touyz RM. Reactive oxygen species, vascular oxidative stress, and redox signaling in hypertension: What is the clinical significance? *Hypertension* 2004; **44:** 248–252.
65. Guzik TJ, West NE, Black E, McDonald D, Ratnatunga C, Pillai R, et al. Vascular superoxide production by NAD(P)H oxidase: Association with endothelial dysfunction and clinical risk factors. *Circ Res* 2000; **86:** E85–E90.
66. Higashi Y, Sasaki S, Nakagawa K, Matsuura H, Oshima T, Chayama K. Endothelial function and oxidative stress in renovascular hypertension. *N Engl J Med* 2002; **346:** 1954–1962.
67. Yamashita N, Hoshida S, Otsu K, Asahi M, Kuzuya T, Hori M. Exercise provides direct biphasic cardioprotection via manganese superoxide dismutase activation. *J Exp Med* 1999; **189:** 1699–1706.

68. Rush JW, Turk JR, Laughlin MH. Exercise training regulates SOD-1 and oxidative stress in porcine aortic endothelium. *Am J Physiol Heart Circ Physiol* 2003; **284:** H1378–H1387.
69. Stralin P, Karlsson K, Johansson BO, Marklund SL. The interstitium of the human arterial wall contains very large amounts of extracellular superoxide dismutase. *Arterioscler Thromb Vasc Biol* 1995; **11:** 2032–2036.
70. Fukai T, Siegfried MR, Ushio-Fukai M, Cheng Y, Kojda G, Harrison DG. Regulation of the vascular extracellular superoxide dismutase by nitric oxide and exercise training. *J Clin Invest* 2000; **105:** 1631–1639.
71. Hornig B, Landmesser U, Kohler C, Ahlersmann D, Spiekermann S, Christoph A, et al. Comparative effect of ace inhibition and angiotensin II type 1 receptor antagonism on bioavailability of nitric oxide in patients with coronary artery disease: Role of superoxide dismutase. *Circulation* 2001; **103:** 799–805.
72. Takeshita S, Inoue N, Ueyama T, Kawashima S, Yokoyama M. Shear stress enhances glutathione peroxidase expression in endothelial cells. *Biochem Biophys Res Commun* 2000; **273:** 66–71.
73. Amano M, Chihara K, Kimura K, Fukata Y, Nakamura N, Matsuura Y, et al. Formation of actin stress fibers and focal adhesions enhanced by Rho-kinase. *Science* 1997; **275:** 1308–1311.
74. Uehata M, Ishizaki T, Satoh H, Ono T, Kawahara T, Morishita T, et al. Calcium sensitization of smooth muscle mediated by a Rho-associated protein kinase in hypertension. *Nature* 1997; **389:** 990–994.
75. Hall A. Rho GTPases and the actin cytoskeleton. *Science* 1998; **279:** 509–514.
76. Kimura K, Fukata Y, Matsuoka Y, Bennett V, Matsuura Y, Okawa K, et al. Regulation of the association of adducin with actin filaments by Rho-associated kinase (Rho-kinase) and myosin phosphatase. *J Biol Chem* 1998; **273:** 5542–5548.
77. Inagaki N, Nishizawa M, Ito M, Fujioka M, Nakano T, Tsujino S, et al. Myosin binding subunit of smooth muscle myosin phosphatase at the cell-cell adhesion sites in MDCK cells. *Biochem Biophys Res Commun* 1997; **230:** 552–556.
78. Mallat Z, Gojova A, Sauzeau V, Brun V, Silvestre JS, Esposito B, et al. Rho-associated protein kinase contributes to early atherosclerotic lesion formation in mice. *Circ Res* 2003; **93:** 884–888.
79. Kataoka C, Egashira K, Inoue S, Takemoto M, Ni W, Koyanagi M, et al. Important role of Rho-kinase in the pathogenesis of cardiovascular inflammation and remodeling induced by long-term blockade of nitric oxide synthesis in rats. *Hypertension* 2002; **39:** 245–250.
80. Rikitake Y, Kim HH, Huang Z, Seto M, Yano K, Asano T, et al. Inhibition of Rho kinase (ROCK) leads to increased cerebral blood flow and stroke protection. *Stroke* 2005; **36:** 2251–2257.
81. Rikitake Y, Oyama N, Wang CY, Noma K, Satoh M, Kim HH, et al. Decreased perivascular fibrosis but not cardiac hypertrophy in ROCK1+/– haploinsufficient mice. *Circulation* 2005; **112:** 2959–2965.
82. Masumoto A, Hirooka Y, Shimokawa H, Hironaga K, Setoguchi S, Takeshita A. Possible involvement of Rho-kinase in the pathogenesis of hypertension in humans. *Hypertension* 2001; **38:** 1307–1310.
83. Masumoto A, Mohri M, Shimokawa H, Urakami L, Usui M, Takeshita A. Suppression of coronary artery spasm by the Rho-kinase inhibitor fasudil in patients with vasospastic angina. *Circulation* 2002; **105:** 1545–1547.
84. Sauzeau V, Le Jeune H, Cario-Toumaniantz C, Smolenski A, Lohmann SM, Bertoglio J, et al. Cyclic GMP-dependent protein kinase signaling pathway inhibits RhoA-induced Ca^{2+} sensitization of contraction in vascular smooth muscle. *J Biol Chem* 2000; **275:** 21722–21729.
85. Shimokawa H. Rho-kinase as a novel therapeutic target in treatment of cardiovascular diseases (Review). *J Cardiovasc Pharmacol* 2002; **39:** 319–327.
86. Shimokawa H, Takeshita A. Rho-kinase is an important therapeutic target in cardiovascular medicine (Review). *Arterioscler Thromb Vasc Biol* 2005; **25:** 1767–1775.
87. Wolfrum S, Dendorfer A, Rikitake Y, Stalker TJ, Gong Y, Scalia R, et al. Inhibition of Rho-kinase leads to rapid activation of phosphatidylinositol 3-kinase/protein kinase Akt and cardiovascular protection. *Arterioscler Thromb Vasc Biol* 2004; **24:** 1842–1847.
88. Noma K, Higashi Y, Jitsuiki D, Hara K, Kimura M, Nakagawa K, et al. Smoking activates rho-kinase in smooth muscle cells of forearm vasculature in humans. *Hypertension* 2003; **41:** 1102–1105.
89. Bailey SR, Mitra S, Flavahan S, Flavahan NA. Reactive oxygen species from smooth muscle mitochondria initiate cold-induced constriction of cutaneous arteries. *Am J Physiol Heart Circ Physiol* 2005; **289:** H243–H250.
90. Jin L, Ying Z, Webb RC. Activation of Rho/Rho kinase signaling pathway by reactive oxygen species in rat aorta. *Am J Physiol Heart Circ Physiol* 2004; **287:** H1495–H1500.
91. Rikitake Y, Liao JK. Rho-kinase mediates hyperglycemia-induced plasminogen activator inhibitor-1 expression in vascular endothelial cells. *Circulation* 2005; **111:** 3261–3268.
92. Noma K, Goto C, Nishioka K, Jitsuiki D, Umemura T, Ueda K, et al. Roles of rho-associated kinase and oxidative stress in the pathogenesis of aortic stiffness. *J Am Coll Cardiol* 2007; **49:** 698–705.

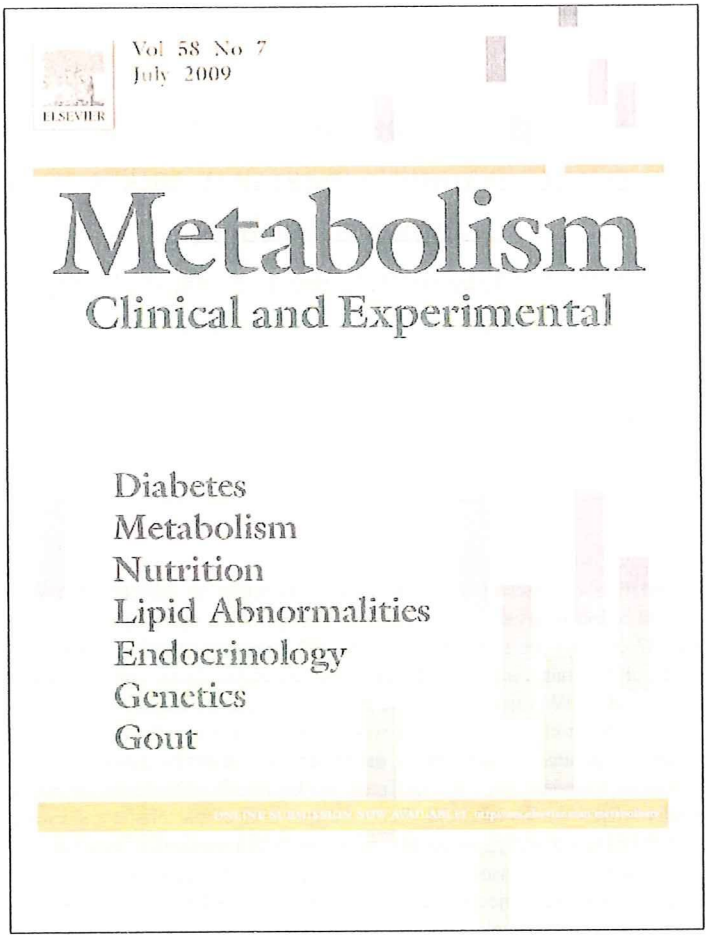

Available online at www.sciencedirect.com

ScienceDirect

Metabolism Clinical and Experimental 58 (2009) 1023–1029

Metabolism
Clinical and Experimental

www.metabolismjournal.com

The impact of visceral adipose tissue and high–molecular weight adiponectin on cardio-ankle vascular index in asymptomatic Japanese subjects

Norihiko Ohashi[a,b,*], Chikako Ito[a], Rumi Fujikawa[a], Hideya Yamamoto[b], Yasuki Kihara[b], Nobuoki Kohno[c]

[a]*Grand Tower Medical Court Life Care Clinic, Hiroshima, Japan*
[b]*Department of Cardiovascular Medicine, Graduate School of Biomedical Sciences, Hiroshima University, Hiroshima, Japan*
[c]*Department of Molecular and Internal Medicine, Graduate School of Biomedical Sciences, Hiroshima University, Hiroshima, Japan*

Received 22 January 2009; accepted 20 March 2009

Abstract

Few studies addressed the relation of visceral adiposity and high–molecular weight (HMW) adiponectin to arterial stiffness. We investigated the impact of visceral adipose tissue (VAT) and HMW adiponectin on cardio-ankle vascular index (CAVI) in asymptomatic Japanese subjects. We studied 487 consecutive subjects (271 men and 216 women) who underwent general health examination between October 2005 and May 2008. The abdominal, visceral, and subcutaneous adipose tissue areas were determined by low-dose x-ray computed tomography. Serum levels of total and HMW adiponectin were measured using the enzyme-linked immunosorbent assay system based on a monoclonal antibody to humans. Cardio-ankle vascular index was positively correlated with VAT area and negatively correlated with HMW adiponectin levels. We also found the positive association of the number of metabolic syndrome components with CAVI in both sexes. A stepwise multiple regression analysis revealed that age, VAT area, serum HMW adiponectin levels, and homeostasis model assessment of insulin resistance were independent determinants of CAVI. Receiver operating characteristic analyses demonstrated that the predictive value of the VAT area for the extent of CAVI (mild: <25th percentile vs severe: >75th percentile) exceeded that of total or HMW adiponectin levels in both sexes. In conclusion, increased CAVI is associated with both amounts of VAT measured by computed tomography and serum HMW adiponectin levels in asymptomatic Japanese subjects. Receiver operating characteristic analysis indicates that the VAT area is a lot better predictor of arterial stiffness than adiponectin levels.

1. Introduction

Visceral adipose tissue (VAT) is now generally considered to play an important role in the metabolic syndrome (MetS) and the development of atherosclerosis [1,2]. The adipose tissue is a remarkable endocrine organ that is a source of several adipokines [3]. Although most adipokines appear to promote cardiovascular disease (CVD), adiponectin is thought to possess antiatherogenic and anti-inflammatory effects and may be protective against CVD development [4]. Recent studies have demonstrated that high–molecular weight (HMW) adiponectin is the major active form of this protein associated with insulin sensitivity and protective activities on the vasculature [5,6]. Clinical studies have also reported that HMW adiponectin is more associated with MetS and coronary heart disease than total adiponectin [7,8], suggesting that HMW adiponectin rather than total adiponectin may exert antiatherosclerotic properties that would prevent the development of atherosclerosis.

It has been demonstrated that aortic pulse wave velocity (PWV), which reflects arterial stiffness, is a marker of CVD risk [9]. Recently, the cardio-ankle vascular index (CAVI) has been developed for the quantitative evaluation of vascular wall stiffness in the aorta, femoral arteries, and tibial artery by measuring PWV and blood pressure (BP) [10]. Indeed, CAVI has been reported to be correlated with

* Corresponding author. Grand Tower Medical Court, Hiroshima 730-0012, Japan. Tel.: +81 82 227 3366; fax: +81 82 227 1666.
E-mail address: [redacted] (N. Ohashi).

0026-0495/$ – see front matter © 2009 Elsevier Inc. All rights reserved.
doi: [redacted]

other CVD risk markers, such as intima-media thickness (IMT) and coronary atherosclerosis, thus reflecting the degree of atherosclerotic change in general populations and patients with high CVD risk [11,12].

Previous studies have reported that visceral adiposity is associated with PWV in patients with type 2 diabetes mellitus [13] or that total adiponectin is inversely related to PWV in patients with essential hypertension [14]. However, there are little data assessing the relationship of visceral adiposity, total adiponectin levels, and HMW adiponectin levels to arterial stiffness in apparently healthy subjects without any medication. Furthermore, it is not known which of these adiposity-related measurements is more closely related to arterial stiffness. The purpose of this study was to evaluate the impact of VAT measured by computed tomography (CT) and total and HMW adiponectin levels on CAVI in asymptomatic Japanese subjects.

2. Methods

2.1. Subjects

The study population consisted of 487 Japanese individuals (271 men, 216 women) who underwent general health examination between October 2005 and May 2008 at Grand Tower Medical Court Life Care Clinic. Subjects who were diagnosed as having CVD and received any medication were excluded. We measured abdominal VAT areas by low-dose x-ray CT, the serum total and HMW adiponectin levels, and the CAVI in all subjects. This study was approved by the Medical Ethics Committee of the Grand Tower Medical Court Life Care Clinic. All subjects provided written informed consent before their inclusions in the study.

2.2. Anthropometric measurement and laboratory methods

After an overnight fast, blood samples were obtained; and BP was measured in the sitting position with the right arm. Height (in meters) and body weight (in kilograms) were used to calculate the body mass index (BMI). The waist circumference (WC) was measured at a level of umbilicus in the late exhalation phase while standing. Measurements of the abdominal VAT and subcutaneous adipose tissue (SAT) areas were undertaken using low-dose x-ray CT with a Hitachi Robusto (Hitachi Medical, Tokyo, Japan). Serum lipid profile was determined by an enzymatic method (total cholesterol and triglycerides) or a direct method (low-density lipoprotein [LDL] cholesterol and high-density lipoprotein [HDL] cholesterol) with a Hitachi 7080 analyzer. The fasting plasma glucose (FPG) levels were measured using the hexokinase method. Serum insulin levels were measured using a chemiluminescent enzyme immunoassay. Insulin resistance was evaluated by the homeostasis model assessment (HOMA-IR), calculated as fasting insulin (in microunits per milliliter) × FPG (in millimoles per liter)/22.5. Hemoglobin A_{1c} (HbA_{1c}) was determined by turbidimetric immunoassay. Serum concentrations of high-sensitivity C-reactive protein (hsCRP) were determined by latex turbidimetric immunoassay. Serum levels of total and HMW adiponectin were measured using the enzyme-linked immunosorbent assay system (Sekisui Medical, Tokyo, Japan) based on a monoclonal antibody to humans [15]. For total adiponectin, the intraassay coefficient of variation (CV) was 4.5% and the interassay CV was 3.0%. For HMW adiponectin, the intraassay CV was 7.7% and the interassay CV was 9.1%. *Metabolic syndrome* was defined by the Japanese criteria as a WC level of at least 85 cm in men and at least 90 cm in women and 2 or more of the following 3 risk factors: hypertension (a BP level ≥130/85 mm Hg), dyslipidemia (an HDL cholesterol level ≤40 mg/dL or a triglycerides level ≥150 mg/dL), and glucose intolerance (an FPG level ≥110 mg/dL) [16]. Metabolic syndrome score (MS) means the number of components of the MetS.

2.3. Measurement of CAVI

Cardio-ankle vascular index was recorded using a VaseraVS-1000 vascular screening system (Fukuda Denshi, Tokyo, Japan) by the methods as previously described [10]. Briefly, cuffs were applied to bilateral upper arms and ankles, electrocardiogram leads were attached to both wrists, and a phonocardiogram was placed at the right sternum border in the second intercostal space. The subjects were placed in the supine position for at least 10 minutes, and then measurements were performed automatically. Cardio-ankle vascular index was calculated by the following formula: $CAVI = a[(2\rho/\Delta P) \times \ln (Ps/Pd)PWV^2] + b$, where Ps is systolic BP, Pd is diastolic BP, ΔP is Ps − Pd, ρ is blood density, and a and b are constants to match aortic PWV. The equation was derived from Bramwell-Hill's equation and the stiffness parameter β. The obtained data were analyzed using VSS-10 software (Fukuda Denshi), and the values of right and left CAVI were calculated. Averages of the right and left CAVI were used in the analysis. The average CV of CAVI has been reported to be 3.8% [10]. The ankle brachial index (ABI) was also calculated as the highest ankle systolic pressure divided by the highest brachial systolic pressure on both sides, and the lower ABI from right and left measurements was used in subsequent statistical analysis.

2.4. Statistical analysis

Categorical variables were presented as number of patients (percentage), and continuous variables were expressed as means ± SD or medians (interquartile range). Differences between men and women in the clinical variables were evaluated using Student t test or the Mann-Whitney U test. The mean CAVI values were stratified by the number of components of MetS using analysis of variance. The correlation coefficient was estimated by

Pearson correlation. As triglycerides, fasting insulin, HOMA-IR, total and HMW adiponectin levels, and hsCRP were not normally distributed, logarithmic transformation was performed for the analysis. We performed stepwise multiple regression analysis to evaluate the independent determinants of CAVI in all subjects using age, sex, BMI, WC, systolic and diastolic BP, triglycerides, HDL cholesterol, LDL cholesterol, FPG, fasting insulin, HOMA-IR, HbA_{1c}, prevalence of MetS, VAT area, SAT area, total adiponectin levels, HMW adiponectin levels, and hsCRP as covariates. A receiver operating characteristics (ROC) analysis was used to compare the predictive power of the VAT area, total adiponectin levels, and HMW adiponectin levels in the prediction of the extent of CAVI. Prediction of CAVI extent was based on discrimination between subjects with mild (CAVI <25th percentile) and severe (CAVI >75th percentile) values of CAVI. Statistical comparisons of the area under ROC curves were performed using a computer program (ROCKIT; Charles E Metz, University of Chicago). Statistical analyses were performed using the JMP 5.0.1 statistical software (SAS Institute, Cary, NC). A P value less than .05 was considered statistically significant.

3. Results

3.1. Patient characteristics

The study subjects consisted of 271 men (mean age, 46 years; range, 23-73 years) and 216 women (mean age, 47 years; range, 25-70 years). The clinical and biochemical characteristics of the study subjects are shown in Table 1. Body mass index, WC, systolic and diastolic BP, triglycerides, LDL cholesterol, FPG, fasting insulin, HOMA-IR, HbA_{1c}, prevalence of MetS, hsCRP, and CAVI were significantly higher in men than in women. The VAT area was also significantly larger in men than in women. High-density lipoprotein cholesterol and the serum total and HMW adiponectin levels were significantly lower in men than in women.

Table 1
Clinical and biochemical characteristics of the study subjects

	Men (n = 271)	Women (n = 216)	P
Age (y)	46.3 ± 10.5	46.6 ± 10.8	NS
BMI (kg/m^2)	24.6 ± 3.9	21.0 ± 3.1	<.01
WC (cm)	87.0 ± 10.6	76.7 ± 8.9	<.01
SBP (mm Hg)	125.9 ± 15.5	116.3 ± 14.1	<.01
DBP (mm Hg)	79.0 ± 10.5	72.0 ± 9.2	<.01
Total cholesterol (mg/dL)	208.4 ± 34.2	207.7 ± 38.7	NS
Triglycerides (mg/dL)	120.0 (80.0-189.0)	66.0 (48.0-93.0)	<.01
HDL cholesterol (mg/dL)	55.6 ± 13.9	70.2 ± 16.7	<.01
LDL cholesterol (mg/dL)	124.7 ± 32.4	118.2 ± 32.8	<.05
FPG (mg/dL)	109.3 ± 23.7	94.6 ± 17.3	<.01
Fasting insulin (μU/mL)	6.8 (4.6-10.8)	4.7 (3.5-6.8)	<.01
HOMA-IR	1.75 (1.11-2.90)	1.07 (0.79-1.57)	<.01
HbA_{1c} (%)	5.38 ± 0.81	5.12 ± 0.60	<.01
MetS (n, %)	81 (29.9)	15 (6.9)	<.01
VAT area (cm^2)	99.3 ± 54.0	38.7 ± 31.2	<.01
SAT area (cm^2)	139.6 ± 73.8	143.6 ± 69.6	NS
Total adiponectin (μg/mL)	4.2 (3.1-5.4)	7.6 (5.8-10.0)	<.01
HMW adiponectin (μg/mL)	1.5 (0.8-2.2)	3.8 (2.4-5.3)	<.01
hsCRP (mg/L)	0.68 (0.37-1.36)	0.33 (0.19-0.68)	<.01
CAVI	7.49 ± 1.03	7.21 ± 0.95	<.01
ABI	1.15 ± 0.1	1.10 ± 0.1	NS

Data are expressed as number of subjects (percentage), means ± SD, or medians (interquartile range). SBP indicates systolic blood pressure; DBP, diastolic blood pressure; NS, not significant.

Table 2
Correlation between CAVI and clinical variables in men and women

Clinical variables	Men (n = 271)		Women (n = 216)	
	r	P	r	P
Age (y)	0.474	<.0001	0.568	<.0001
BMI (kg/m^2)	0.048	.42	−0.08	.23
WC (cm)	0.046	.44	0.071	.29
SBP (mm Hg)	0.183	.0025	0.185	.0064
DBP (mm Hg)	0.121	.046	0.184	.0067
Total cholesterol (mg/dL)	−0.038	.53	0.164	.015
Triglycerides (mg/dL)[a]	0.0756	.21	0.25	.0002
HDL cholesterol (mg/dL)	−0.034	.57	−0.115	.091
LDL cholesterol (mg/dL)	−0.049	.41	0.186	.0061
FPG (mg/dL)	0.232	.0001	0.236	.0005
Fasting insulin (μU/mL)[a]	0.211	.0007	0.238	.0005
HOMA-IR[a]	0.260	<.0001	0.284	<.0001
HbA_{1c} (%)	0.232	.0001	0.282	<.0001
VAT area (cm^2)	0.366	<.0001	0.383	<.0001
SAT area (cm^2)	0.15	.013	0.154	.023
Total adiponectin (μg/mL)[a]	−0.113	.061	−0.09	.18
HMW adiponectin (μg/mL)[a]	−0.254	.0001	−0.214	.0021
hsCRP (mg/L)[a]	0.173	.0041	0.112	.1
ABI	0.122	.06	0.091	.2

Abbreviations are the same as in Table 1.
[a] Log-transformed values.

3.2. Correlation between CAVI and clinical variables

Table 2 shows the result of simple linear regression analysis between CAVI and clinical variables. Cardio-ankle vascular index was positively correlated with age, systolic and diastolic BP, FPG levels, fasting insulin, HOMA-IR, HbA_{1c} levels, VAT area, and SAT area and negatively correlated with HMW adiponectin levels in both sexes. Cardio-ankle vascular index was positively correlated with hsCRP in men and with total cholesterol, triglycerides, and LDL cholesterol in women. Fig. 1 shows the comparison of CAVI values according to the MS in men and women. In both sexes, CAVI increased linearly as the MS increased; average CAVI values for those with MS of 0, 1, 2, or at least 3 were 7.13, 7.27, 7.53, and 7.92 in men (P for trend < .0001) and 7.05, 7.32, 7.62, and 8.18 in women (P for trend < .0001), respectively. In addition, subjects with MetS had a significantly higher CAVI than those without in men ([mean ± SD] 7.91 ± 1.0 vs 7.31 ± 0.98, P < .001) and women (8.18 ± 1.54 vs 7.15 ± 0.82, P < .001). Table 3 describes the result of stepwise multiple regression analysis in all subjects. Age, VAT area, HMW adiponectin levels,

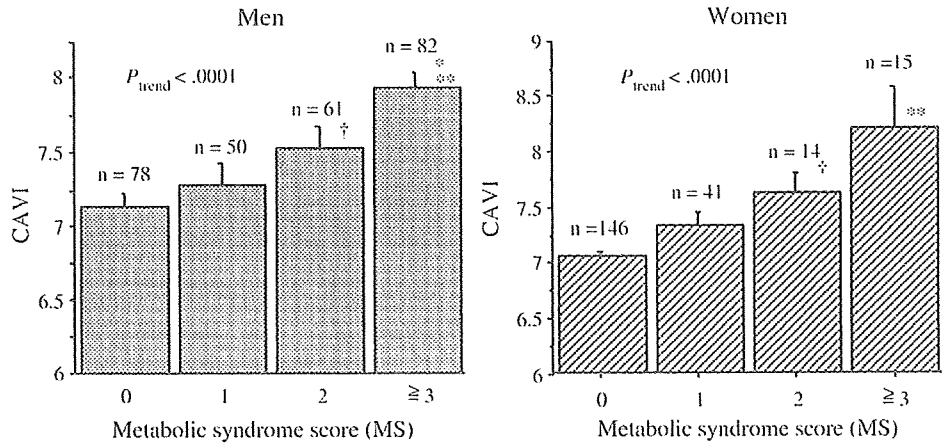

Fig. 1. Comparison of CAVI values according to the MS in men and women. MS means the number of components of the MetS including WC, BP, triglycerides or HDL cholesterol, and FPG. †P less than .05 vs MS = 0 group, *P less than .05 vs MS = 2 group, **P less than .01 vs MS = 0 or MS = 1 group in men, †P less than .05 vs MS = 0 group, **P less than .01 vs MS = 0 or MS = 1 group in women.

and HOMA-IR were found to be independent determinants of CAVI (adjusted R^2 = 0.38, P < .0001).

3.3. Predictive values of the VAT area, total adiponectin levels, and HMW adiponectin levels for the extent of CAVI

Receiver operating characteristic analyses were performed to quantify the power of the VAT area, total adiponectin levels, and HMW adiponectin levels for the prediction of CAVI extent (Fig. 2). Analyses were performed in subjects representing the upper (n = 66, CAVI >8.05 in men; n = 52, CAVI >7.70 in women) and lower quartile (n = 67, CAVI <6.80 in men; n = 50, CAVI <6.60 in women) of CAVI. The area under the curve for the VAT area was significantly larger than that for HMW adiponectin levels in men (VAT area: 0.763 [95% confidence interval {CI}, 0.676-0.836] vs HMW adiponectin levels: 0.653 [95% CI, 0.556-0.741], P = .05) and women (VAT area: 0.762 [95% CI, 0.670-0.837] vs HMW adiponectin levels: 0.627 [95% CI, 0.524-0.720], P = .02). The area under the curve for HMW adiponectin levels was also significantly larger than that for total adiponectin levels in men (HMW adiponectin levels: 0.653 [95% CI, 0.556-0.741] vs total adiponectin levels: 0.583 [95% CI, 0.485-0.677], P = .03) and women (HMW adiponectin levels: 0.627 [95%, CI 0.524-0.720] vs total adiponectin levels: 0.538 [95% CI, 0.436-0.638], P = .01).

Table 3
Stepwise multiple regression analysis between CAVI and clinical variables

Independent variables	Standardized β	Standard error	t	P
Age	1.47	0.12	12.4	<.0001
VAT area	0.46	0.18	2.62	.0092
HMW adiponectin[a]	−0.54	0.26	−2.10	.036
HOMA-IR[a]	1.52	0.76	2.00	.046
R^2	0.40			
Adjusted R^2	0.38			

Abbreviations are the same as in Table 1.
[a] Log-transformed values.

4. Discussion

In the present study, we first evaluated the association of the VAT area, total adiponectin levels, and HMW adiponectin levels with CAVI as a marker of arterial stiffness in a group of subjects without previous manifestation of CVD. We found a positive association of MetS components and VAT area with CAVI. We also found an inverse relation between HMW adiponectin levels and CAVI. A stepwise multiple regression analysis revealed that age, VAT area, HMW adiponectin levels, and HOMA-IR were independent predictors for increase of CAVI. On ROC analysis, VAT area demonstrated superior discrimination for the extent of CAVI compared with total and HMW adiponectin levels in both sexes.

We showed that CAVI is higher in subjects with MetS than in those without and increased linearly as the components of MetS increased, which is consistent with prior result that MetS is independently associated with arterial stiffness [17]. Previous studies also reported that the VAT area is significantly associated with arterial stiffness in older adults [18], middle-aged women [19], and patients with type 2 diabetes mellitus [13]. With respect to total adiponectin and arterial stiffness, there is a significant relationship in hypertensive patients [14] and nondiabetic subjects [20]. However, there has been no information regarding the effect of VAT and HMW adiponectin levels on arterial stiffness in asymptomatic subjects. We found that both the VAT area and HMW adiponectin levels remained as independent determinants of CAVI in multivariable analysis even after adjustment for MetS or other indices of adiposity measurement such as BMI, SAT, and WC. These results indicate that the measurement of the VAT area and HMW

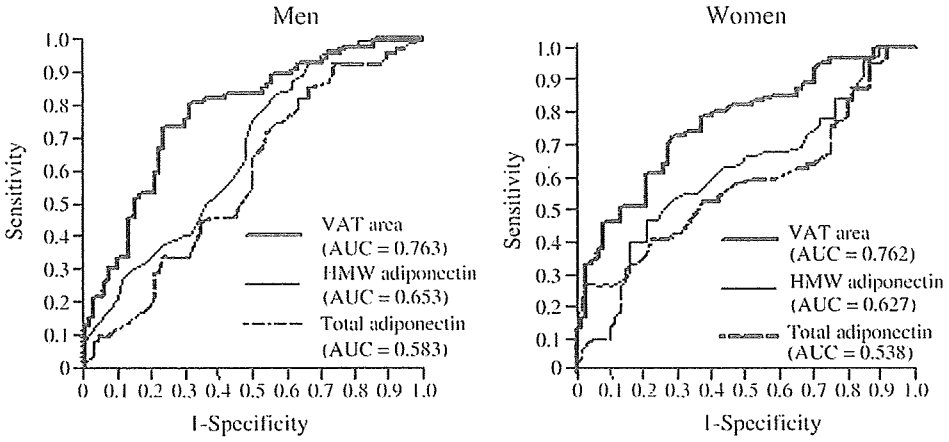

Fig. 2. Receiver operating characteristic curves of the VAT area, total adiponectin levels, and HMW adiponectin levels and predictive values for the extent of CAVI in men and women.

adiponectin levels in conjugation with CAVI may help identify subjects needing more aggressive risk modification in clinical practice.

The mechanisms of linking VAT and adiponectin to arterial stiffness are not entirely understood. In the present study, we demonstrated that HOMA-IR as a marker of insulin resistance was an independent predictor of CAVI, which implies one of the plausible mechanisms of increased arterial stiffness. Arner [21] has suggested that the flux of lipid from the visceral fat to the liver via portal circulation might account for hepatic insulin resistance. Adiponectin was also reported to modulate insulin sensitivity by stimulating glucose utilization and fatty acid oxidation via the phosphorylation and activation of adenosine monophosphate–activated protein kinase in both muscle and liver cells [22]. Clinical study also suggests that HMW adiponectin is a more useful marker to evaluate insulin resistance and MetS than total adiponectin [7]. Insulin resistance is reported to be associated with decreased endothelium-dependent vasodilation [23] and increased arterial stiffness [24]. These results indicated that decreased HMW adiponectin levels concomitant with the accumulation of visceral fat could potentially be involved with the acceleration of the increased arterial stiffness via insulin resistance.

From ROC analysis, we can clearly see that the VAT area was a lot better predictor of arterial stiffness than adiponectin levels. The accumulation of VAT is considered to be causally linked to atherosclerosis as a result of the dysregulation of various kinds of adipokines production and chronic intravascular inflammation [5]. Our findings suggested that other factors than adiponectin, such as inflammatory factors, other proteins secreted by adipose tissue, or insulin or glucose levels may also be important in the pathophysiologic mechanisms by which abdominal adiposity leads to arterial stiffness. In addition, HMW adiponectin was more associated with arterial stiffness than total adiponectin. One possible explanation of this result may be the higher affinity of HMW adiponectin to collagen in the vascular wall compared with low–molecular weight or middle–molecular weight forms, thus possibly exerting better repair on injured vessels [25]. In addition, a recent study revealed that only HMW adiponectin selectively suppressed endothelial cell apoptosis, whereas neither the low–molecular weight nor the middle–molecular weight form had this effect [6]. Clinical data also confirmed that HMW to total adiponectin ratio was an independent determinant for PWV and CAVI in hemodialysis patients [26].

In the present study that represents arterial stiffness by CAVI, neither BP nor sex remained as independent predictors of CAVI in stepwise multiple regression analysis. Whereas BP is a major determinant of PWV, CAVI is designed to be adjusted for BP based on the stiffness parameter β and is hypothesized to measure arterial stiffness independent of BP. It has been reported that CAVI has a lower correlation with BP than PWV [10] or that the significant risk factors of high CAVI were age and HbA_{1c}, whereas systolic BP was not relevant [27], which is consistent with our results in that BP did not contribute to CAVI. In addition, there was no significant sex interaction in our analyses. For instance, menopause is reported to augment the age-related increase in arterial stiffness [28]. However, our study subjects are relatively young and the proportion of postmenopausal women is low, which may be one of the reasons that CAVI was not affected by sex in a multivariable model.

This study had some limitations. First, because this is a cross-sectional study, causality cannot be established. However, it bas been already reported that arterial stiffness defined by stiffness parameter β is partly improved by interventions to insulin resistance such as the insulin sensitizer pioglitazone and aerobic exercise in type 2 diabetes mellitus [29,30]. Our findings in the present study are almost in keeping with these previous observations,